Communications Medicine

https://doi.org/10.1038/s43856-026-01628-0

Article in Press

Climate and socioeconomic factors drive heterogeneous dengue risk escalation in the Chinese population

Received: 13 November 2025

Accepted: 21 April 2026

Cite this article as: Guang, X., He, Y., Geng, M. *et al.* Climate and socioeconomic factors drive heterogeneous dengue risk escalation in the Chinese population. *Commun Med* (2026). https://doi.org/10.1038/s43856-026-01628-0

Xu Guang, Yifei He, Mengjie Geng, Meifang Liu, Jia Wan, Dongfeng Kong, Zhen Zhang, Lanbin Xiang, Liangqiang Lin, Rongxin He, Ning Zhang, Felipe Arley Costa Pessoa, Claudia Maria Ríos Velasquez, Carolina Mercedes Laurent Singh, Pritesh Lalwani, Jie Huang, Haidong Wang, Jue Liu & Bin Zhu

Climate and socioeconomic factors drive heterogeneous dengue risk escalation in the Chinese population

Xu Guang[1#], Yifei He[1#], Mengjie Geng[2#], Meifang Liu[1], Jia Wan[3], Dongfeng Kong[3], Zhen Zhang[3], Lanbin Xiang[3], Liangqiang Lin[3], Rongxin He[4], Ning Zhang[5], Felipe Arley Costa Pessoa[6], Claudia Maria Ríos Velasquez[6], Carolina Mercedes Laurent Singh[6], Pritesh Lalwani[6], Jie Huang[1], Haidong Wang[1], Jue Liu[7*], Bin Zhu[1*]

[1]School of Public Health and Emergency Management, Southern University of Science and Technology, Shenzhen, China.

[2]Chinese Center for Disease Control and Prevention, Beijing, China.

[3]Shenzhen Center for Disease Control and Prevention, Shenzhen, China.

[4]School of Health Management, Southern Medical University, Guangzhou, China.

[5]Vanke School of Public Health, Tsinghua University, Beijing, China.

[6]Instituto Leoônidas e Maria Deane, Fiocruz Amazoônia, Manaus, Brazil.

[7]School of Public Health, Peking University, Haidian District, Beijing, China.

*Corresponding author:

Jue Liu, School of Public Health, Peking University, Haidian District, Beijing, China. 100871, jueliu@bjmu.edu.cn.

Bin Zhu, School of Public Health and Emergency Management, Southern University of

Science and Technology, Shenzhen, China. 518055, zhub6@sustech.edu.cn.

[#] These authors contributed equally to this work.

Abstract

Background

Dengue risk is increasingly shaped by climate change and rapid urbanization, yet comprehensive, multidimensional risk assessments grounded in a One Health perspective remain scare.

Methods

We develop a geographically eXplainable artificial intelligence (GeoXAI) model to estimate dengue hazard across China in 2024 (current), 2050, and 2100 under different shared socioeconomic pathway (SSP) scenarios. A hazard-exposure-vulnerability framework is then used to assess dengue risk by integrating dengue hazard, human exposure, and social vulnerability.

Results

Here we show a northward expansion of high-hazard areas, with the minimum temperature in the coldest month being the dominant driver (27.2% contribution). Moreover, socioeconomic factors such as population density (3.8%) and urbanization level (2.7%) will further amplify dengue hazard. Current dengue risk assessments reveal high-risk clusters in Southwest China and megacities. Dengue risk exhibits spatially heterogeneous escalation in the future, with Southwest and Southeast China facing the steepest growth and Northwest China experiencing disproportionate increases.

Compared to the current, dengue risk in SSP585—a high greenhouse gas emission scenario and limited climate policy interventions—increases by 6.01% (2050) and 8.21% (2100), representing the largest escalation among the three SSPs.

Conclusions

Despite ongoing disease control efforts, our findings underscore the need to intensify integrated surveillance and multidimensional intervention strategies against escalating dengue risk in China, and offers lessons for other prevalent *Aedes*-borne diseases (e.g., chikungunya).

Plain language summary

Dengue is a vector-borne infectious disease mainly transmitted by mosquitoes, which poses a growing public health concern in China. Understanding where and why this risk is growing is essential for effective prevention. In this study, we developed a multi-dimensional risk assessment framework that combines three key factors: dengue hazard, human exposure, and social vulnerability. Our findings show that high-risk areas are mainly concentrated in southern and southwestern China, with clear spatial differences in risk distribution. We found that increased contact between humans and mosquitoes and rapid urbanization are driving dengue risk across urbanized regions under climate change. In the future, the overall risk intensity is expected to increase unevenly. While high-risk clusters will remain stable in the south, new risk hotspots are likely to emerge in

northern areas. Our results show that fighting dengue requires strategies that combine climate adaptation with improved urban planning.

Introduction

Dengue is an arboviral disease primarily transmitted to humans through the bite of infected *Aedes* mosquitoes[1,2]. According to the World Health Organization (WHO), the global incidence has increased exponentially over the past few decades[3], with reported cases increasing tenfold from 0.5 to 5 million between 2000 and 2023[4,5,6]. This trend peaked in 2024, with reported cases exceeding 12 million, including more than 8000 dengue-related deaths[7,8]. As the world's second-most populous and one of the fastest-urbanizing country, China faces an increasingly severe public health threat from dengue[1].

The habitat suitability of *Aedes* mosquitoes (e.g., *Aedes aegypti* and *Aedes albopictus*), which are the main vectors of dengue transmission, is a well-established driver of dengue hazard (i.e., dengue transmission probability), and is significantly modulated by climate change[9,10]. Specifically, climate change-driven shifts, such as rising temperatures and altered precipitation patterns, threaten dengue expansion by altering habitat suitability[11,12]. However, the dynamics of dengue transmission are not governed solely by climate and vector ecology. Socioeconomic factors, particularly the level and pace of urbanization, also affect transmission dynamics[13,14]. In China, socioeconomic change has emerged as a key driver of the gradual northward expansion of high-hazard areas of dengue, with unplanned urbanization increasing dengue transmission through increases in the population density, changes in land use, and strain on water and sanitation infrastructure. Despite the recognition of these key drivers, quantifying the precise influence of climate factors and rapid urbanization on dengue hazard remains

challenging because of the complex and multiple interactions among driving factors[15–17]. The spatially heterogeneous characteristics of these drivers (e.g., socioeconomic disparities and climate thresholds associated with vector patterns) complicate localized impact assessments, necessitating fine-scale modeling to inform regional prevention and control strategies[18–20].

Existing research often relies solely on the regional dengue hazard to characterize population-level risk[21]. However, the regional dengue hazard merely defines the biophysical potential for transmission[22,23]. Whether this potential translates into actual public health threats depends on the number of people living in or visiting high-hazard areas of dengue (i.e., the level of human exposure), with stark contrasts in exposure between densely populated cities and sparsely inhabited rural regions[24,25]. Applying the Intergovernmental Panel on Climate Change (IPCC) conceptual framework, dengue risk involves a complex interplay among multiple dimensions—dengue hazard, human exposure, and social vulnerability[21]. The capacity of socioeconomic systems to withstand or recover from dengue-related outbreaks (i.e., social vulnerability) should not be overlooked either, encompassing factors such as healthcare accessibility and demographic traits such as population aging[26,27]. Failure to account for human exposure and social vulnerability in risk assessment systems may render dengue prevention policies disconnected from real-world dynamics, leading to inefficient allocation of prevention resources.

The specific objectives of this study were fourfold: (i) to develop a geographically

eXplainable artificial intelligence (GeoXAI) model (namely, the geographic neural network weighted logistic regression-Shapley Additive Explanations (GNNWLR-SHAP) model) to estimate the regional dengue hazard level in three periods (current, 2050, and 2100) based on the recently complied *Aedes* vector data and dengue cases across China; (ii) to precisely quantify the effects of climate and socioeconomic factors on the regional dengue hazard across China; (iii) to build a hazard-exposure-vulnerability framework based on the Intergovernmental Panel on Climate Change (IPCC) framework for a comprehensive assessment of dengue risk in China; and (iv) to project the spatial patterns of dengue risk under alternative future climate and socioeconomic development pathways. Ultimately, this study aims to provide multidimensional theoretical underpinnings and actionable guidance for dengue prevention and control systems, thereby facilitating the advancement and local adaptation of the Healthy China Initiative.

This study reveals a northward expansion of high-hazard areas for dengue in China, driven predominantly by the minimum temperature in the coldest month. Socioeconomic factors, including population density and urbanization level, further amplify this risk. Currently, high-risk clusters are concentrated in Southwest China. Projections show a spatially heterogeneous escalation of risk in the future, with the steepest growth anticipated in Southwest and Southeast China and a disproportionate increase in Northwest China. Under the high-emission scenario (SSP585), the risk increase is the largest among all scenarios. These findings underscore the urgent need to intensify integrated surveillance and multi-dimensional intervention strategies to counter the

escalating dengue threat in China.

Methods

Ethics statement

This study complies with all relevant ethical regulations. Ethics approval was obtained from the institutional review board of Southern University of Science and Technology (Ethical Approval No. IRB#2025PES190).

Data collection and preprocessing

Dengue case records and collection of *Aedes albopictus* and *Aedes aegypti* data in China.

Dengue case records and collection of *Aedes albopictus* and *Aedes aegypti* data in China. Dengue case records are openly available at https://doi.org/10.5281/zenodo.7765309. We firstly integrated occurrence records of *Aedes albopictus* and *Aedes aegypti* in China from previously collated databases (doi:10.5061/dryad.47v3c[9], doi.org/10.1186/s40249-023-01083-2[45], and doi.org/10.1016/j.scitotenv.2019.01.301[46]). Then, the previously are updated through the following two sources: (1) We conducted a literature search using the Web of Science (www.isiknowledge.com), China National Knowledge Infrastructure (www.cnki.net), and Wanfang Data (www.wanfangdata.com.cn/index.html) databases to update the existing database for the period 2020–2024 (last updated on 31 November 2024), using the keywords **Aedes** OR **albopictus** OR **aegypti** AND **China** (Table

S8); and (2) We screened out occurrence records with clear taxonomic identities for *Aedes albopictus* and *Aedes aegypti* from the Global Biodiversity Information Facility (GBIF) (http://www.gbif.org) as of December 2024. Subsequently, for data cleaning and integration, we removed duplicate records across the previously collated databases, the updated 2020–2024 literature-derived data, and the GBIF-sourced records, verified that all occurrence coordinates fell within China, confirmed the accuracy of taxonomic identities for *Aedes albopictus* and *Aedes aegypti* to avoid misclassification (Supplementary Note 1, Table S7). In total, the final database included 65 occurrence points for *Aedes aegypti* and 463 occurrence points for *Aedes albopictus*.

Collection and preprocessing of factors. The selection of driving factors for estimating dengue hazard was based on the mechanistic understanding of dengue transmission ecology, which is jointly driven by climate suitability for vector survival, socioeconomic factors influencing human-vector contact, topographic constraints on microclimate, and the habitat suitability of *Aedes* vectors (Supplementary Note 2). Specifically, we selected eleven factors to estimate the regional dengue hazard level[9,10,12]. These factors were chosen to reflect the drivers known to be relevant to dengue transmission in China, for which it was feasible to collect data or derive proximate measures for the baseline year (2024) and project these measures to 2050 and 2100 under different SSPs, including SSP126, SSP245, and SSP585 (Supplementary Table S5). The resulting set of factors was as follows: (1) minimum temperature in the coldest month (bio6); (2) habitat suitability

of *Aedes albopictus*; (3) habitat suitability of *Aedes aegypti*; (4) precipitation in the wettest month (bio13); (5) annual mean temperature (bio1); (6) population density (POP); (7) annual precipitation (bio12); (8) digital elevation model (DEM); (9) impervious surface area (ISA); (10) precipitation in the driest month (bio14); and (11) maximum temperature in the warmest month (bio5). All the factors were obtained or generated at a 5 km × 5 km resolution (Supplementary Table S6).

Statistics and reproducibility

The GNNWLR-SHAP model was used to estimate the dengue hazard throughout China based on either current or projected scenarios of climatic, biological, and socioeconomic factors. We considered the environmental conditions projected at two time points (2050 and 2100) under SSP126, SSP245, and SSP585, which reflect the evolution of global warming based on different trajectories of greenhouse gas concentrations in the atmosphere. To investigate how high-hazard areas of dengue could undergo substantial changes and expand, we considered climatic, topographic, socioeconomic impacts, and the habitat suitability of *Aedes* vectors from 2050 to 2100 to estimate the spatial pattern of dengue hazard levels across China in the future.

GNNWLR model. The GNNWLR model, which is a combination of GNNWR[47,48] and logistic regression (LR), is defined as follows:

$$y(u_i,v_i)=\frac{1}{1+e^{-\left[w_0(u_i,v_i)\times\beta_0+\sum_{k=1}^{p}w_k(u_i,v_i)\times\beta_k\times x_k(u_i,v_i)\right]}} \quad (1)$$

Then, by substituting the β_k values estimated via ordinary least squares into the definition of the GNNWLR model, $y(u_i,v_i)$ can be determined[49]:

$$y(u_i,v_i)=\frac{1}{1+e^{-\sum_{k=0}^{p}w_k(u_i,v_i)\times\beta_k\times x_k(u_i,v_i)}}=\frac{1}{1+e^{-x(u_i,v_i)^{\mathrm{T}}W_{\mathrm{SWNN}}(u_i,v_i)\left(X^{\mathrm{T}}X\right)^{-1}X^{\mathrm{T}}y}} \quad (2)$$

The training of the GNNWLR model is based on the minibatch stochastic gradient descent algorithm, and the loss function is based on binary cross-entropy (BCE). The BCE was expressed as follows[50]:

$$J_{bce}=-\frac{1}{M}\sum_{m=1}^{M}\left[y_m\times\log\left(h_\theta\left(x_m\right)\right)+\left(1-y_m\right)\times\log\left(1-h_\theta\left(x_m\right)\right)\right] \quad (3)$$

where M is the number of training examples m; y_m is the target label for training example m; x_m is the input for training example m; and h_θ is a model with weight θ. Incorporating the GNNWLR along with BCE values, the model converges rapidly and achieves excellent estimation results (Fig. S16).

For each data point (including dengue cases and background points) with geographic coordinate information and driving factors, the procedure entailed the calculation of the geographic distance between the coordinates of the data point and those of other data points within the training dataset. This vector was input into the neural network with dropout-regularized hidden layers (to avoid overfitting), outputting a spatial weight vector. Then, the spatial weight vector undergoes a dot product with coefficients derived from ordinary least squares regression and the driving factor values, followed by a sigmoid

function to calculate the estimated dengue hazard. A BCE function calculated the loss to guide neural network adjustments via negative feedback. The five-fold cross-validation was employed in the GNNWLR model to assess the performance. Relative uncertainty of dengue hazard under different future scenarios was presented in Supplementary Note 3 (Fig. S17).

GNNWLR-SHAP model. The SHAP model provides a local explanation for each sample and offers a global explanation based on the mean Shapley value. The Shapley value for the auxiliary variable X_j was calculated as follows[51]:

$$Shapley\left(X_j\right)=\sum_{S\subseteq N\setminus\{j\}}\frac{k!\left(p-k-1\right)!}{p!}\left[f\left(S\cup\{j\}\right)-f\left(S\right)\right] \quad (4)$$

where p is the total number of auxiliary variables, $N\setminus\{j\}$ is a set of all possible combinations of auxiliary variables, excluding X_j, S is a feature set in $N\setminus\{j\}$, $f(S)$ is the model estimate with auxiliary variables in S, and $f(S\cup\{j\})$ is the model estimate with auxiliary variables in S plus X_j. The Shapley value quantifies the influence of auxiliary variables on a target variable. The locally additive variable attributions are used to generate the interpretable SHAP model, which is defined as follows:

$$y(u_i,v_i)=shap_0(u_i,v_i)+shap\left[X_1(u_i,v_i)\right]+shap\left[X_2(u_i,v_i)\right]+\ldots+shap\left[X_p(u_i,v_i)\right] \quad (5)$$

where $shap_0(u_i,v_i)$ is the mean estimation value across all locations, and $shap\left[X_j(u_i,v_i)\right]$ is the Shapley value of the j-th feature at location (u_i,v_i), which quantifies the influence of the j-th feature on the estimation $y(u_i,v_i)$.

The Shapley value at location (u_i, v_i) for the *j*-th feature in the GNNWLR-SHAP model was calculated as follows:

$$shap\left[X_j(u_i,v_i)\right] = \frac{1}{1+e^{-\sum_{k=0}^{p} w_k(u_i,v_i)\times\beta_k\times x_k(u_i,v_i)}} - \frac{1}{1+e^{-\sum_{k=0,k\neq j}^{p} w_k(u_i,v_i)\times\beta_k\times x_k(u_i,v_i)}} \quad (6)$$

To integrate dynamic data such as international travel flows and domestic migrant population trajectories, we construct the multi-scale mobility quantification models (Supplementary Note 4, Fig. S18-S20). Besides, due to the dengue data in China should suffer from substantial sampling bias, our research methodology framework involves the development of two independent models: a surveillance model and a dengue hazard model (Supplementary Note 5, Fig. S21, and Table S8).

Accuracy assessment. To evaluate the GNNWLR-SHAP model's performance, we employed the area under the receiver operating characteristic curve (AUC), accuracy (ACC), and recall as evaluation indicators[49]:

$$Recall = TPR = \frac{T_p}{R_p} \quad (7)$$

$$FPR = \frac{F_p}{R_n} \quad (8)$$

$$AUC = \int_{x=0}^{1} TPR\left[FPR^{-1}(x)\right]dx \quad (9)$$

$$Accuracy = \frac{T_p + T_n}{R_p + R_n} \quad (10)$$

where T_P and T_N are the numbers of true positives and true negatives, respectively; F_P is the number of false positives; and R_P and R_n are the numbers of truly positive and

negative examples, respectively. Recall is the proportion of positive cases that a classifier accurately identifies among all actual positive cases.

Generation of background samples. The GNNWLR-SHAP model adopts a typical "presence-background" modeling method. We randomly generated background points (absence) across the study area to supplement the observed “presence” points (disease occurrence points). These background points represented areas where we assumed that dengue did not occur, in contrast to the presence points. To reduce the label imbalance, which may lead to issues in subsequent analysis steps, the number of selected background points was set in proportion to the number of dengue occurrence points, maintaining a 1:1 ratio between them[52].

Field validation

To conduct a rigorous validation of the GNNWLR-SHAP model for dengue hazard prediction, Shenzhen City, a typical dengue epidemic hotspot in southern China, was selected for targeted field validation. Shenzhen is a core international port city with intensive cross-border and domestic population mobility, high habitat suitability for *Aedes* mosquito, and frequent local outbreaks. Such a representative epidemic scenario provides an ideal basis to rigorously verify the predictive accuracy of our model. Specifically, we collected and authenticated the reported dengue case data of Shenzhen in 2024 through official collaboration with the Shenzhen CDC. Meanwhile, the values of

key decisive driving factors corresponding to actual dengue occurrence locations, including meteorological conditions, *Aedes* mosquito habitat suitability, population density and human mobility, were extracted and further quantitatively analyzed.

Dengue risk assessment

Framework. As defined by the Intergovernmental Panel on Climate Change (IPCC), risk is a function of hazard, exposure, and vulnerability (Fig. S8). The dengue risk index was derived via the equal-weight aggregation of three components obtained with the minimum–maximum normalization method [53,54]:

$$HHRI_i = \frac{1}{3}\left(HI_i + EI_i + VI_i\right) \tag{11}$$

where *HI*, *EI*, and *VI* are the indices of the dengue hazard, human exposure, and social vulnerability levels, respectively, and *i* is the number of counties (2891). After the risk index was obtained, we standardized the risk values to the range of 0 to 1. The standardized values were divided into five levels: very high (0.80 ≤ risk < 1.00), high (0.60 ≤ risk < 0.80), moderate (0.40 ≤ risk < 0.60), low (0.20 ≤ risk < 0.40), and very low (0.00 ≤ risk < 0.20). This classification helped clearly indicate the level of dengue risk and support targeted prevention and control strategies.

Dengue hazard and human exposure. With the average dengue hazard and population density of each county as the data foundation, we computed the dengue hazard index

and human exposure index, respectively. To guarantee comparability among the exposure index, hazard index, and vulnerability index, we normalized these indices to the 0–1 range via the min–max normalization method. These indices were then categorized using the same five-level qualitative scale.

Social vulnerability index. According to the assessment framework, the vulnerability index encompasses sensitivity and capacity [21]. Sensitivity indicates the susceptibility of people to dengue. Research has shown that social factors such as population structure, socioeconomic status, and the conditions of the residential environment can influence dengue risk. Residential conditions, such as housing stability and high access to sanitation facilities, play key roles in shaping mosquito breeding environments and dengue transmission risks. Other socioeconomic indicators also matter; regions with high educational levels and employment trends are associated with better ability to adopt protective behaviors and access healthcare than are other areas. Some studies have suggested that attributes of the living environment, such as the availability of basic household facilities, can serve as proxies for *Aedes* vector control and the estimation of living standards. Considering the availability and relevance of the data, a set of representative indicators was finally selected to construct the dengue vulnerability index (Table S3). Capacity indicates whether people can address the adverse effects of dengue occurrence by adjusting their own socioeconomic conditions, mainly emphasizing the response to dengue occurrence. Specifically, in this study, capacity was measured based

on the percentage of households with tap water in their houses, the percentage of households with kitchen/lavatory/bathing facilities in their houses, and the percentage of those owning family cars.

Geographically weighted principal component analysis (GWPCA) was applied to extract the main components among the indicators. Geographically weighted principal components (GWPCs) with local eigenvalues above one were retained for varimax rotation to derive orthogonal factors[55]. The social vulnerability index was computed by aggregating the product of each factor score weighted by the corresponding percentage of total variation. Finally, the vulnerability index was similarly standardized to a 0 to 1 range and classified via a five-level qualitative scale.

Results

Likely expansion of high-hazard areas of dengue

The baseline estimates identified high-hazard areas of dengue across southeastern and southwestern China, predominantly distributed in Yunnan, Guangdong, Hainan, and Taiwan, indicating a higher likelihood of dengue occurrence in these regions (Fig. 1f). The high accuracy (AUC = 0.836) demonstrated the superior ability of the GNNWLR-SHAP model to estimate the regional dengue hazard in unknown areas (Supplementary Table S1). In the different future scenarios, the high-hazard areas of dengue consistently expand toward higher latitudes (30°N–35°N) (Fig. 1i). Moreover, the high-hazard areas of dengue may substantially be projected to expand under SSP126, SSP245, and SSP585

(Fig. 2 and Fig. S3). By 2050, the high-hazard areas are expected to become more extensive in East China, Central South China, and Southwest China under all SSP scenarios, with the greatest growth occurring in the SSP585 scenario in Central South China (68.85×10^4 km^2) (Fig. 2a-c). The changes in high-hazard areas predicted for 2050 and 2100 in the SSP126 scenario were less pronounced than those in the SSP245 and SSP585 scenarios, indicating fewer extreme changes in the high-hazard areas of dengue in the sustainable development scenario (SSP126) (Supplementary Figs. S1-S3). The predictions for 2100 revealed a similar growth pattern to that in 2050 but with smaller increases in high-hazard areas, indicating a gradual stabilization of expansion trends compared with the growth in 2050 (Fig. 2d-g). In addition, the mean levels of dengue hazard in Shanghai (53.20%), Hunan (68.92%), Jiangxi (71.97%), Jiangsu (119.72%), and Anhui (150.09%) provinces showed the largest relative increases compared with the current period (Supplementary Table S2).

Drivers of regional dengue hazard levels

We found that the regional dengue hazard was contingent on complex interactions among biological, climatic, topographic, and socioeconomic drivers (Supplementary Fig. S4). The minimum temperature in the coldest month (bio6) emerged as the most important factor related to the regional dengue hazard (27.2%) (contribution to modeled variations: habitat suitability of *Aedes albopictus*, 23.5%; habitat suitability of *Aedes aegypti*, 17.8%; precipitation in the wettest month (bio13), 6.5%; annual mean

temperature (bio1), 3.9%; population density (POP), 3.8%; urbanization level (ISA), 2.7%), as revealed by the Shapley values of the average marginal contributions of corresponding factors based on cooperative game theory. Moreover, this influence was further modulated by interactions with other environmental conditions.

The SHAP total effect patterns revealed how the regional dengue hazard varied with different driving factors (Figs. 3a–c and Supplementary Fig. S5). With the increase in the minimum temperature in the coldest month, the total effect was negative at low levels and transitioned to a positive effect after a tipping point at approximately 0°C. Moreover, the habitat suitability of *Aedes albopictus* and *Aedes aegypti* showed initially negative effect that gradually transitioned to positive effects beyond suitability thresholds of approximately 0.6 for *Aedes albopictus* and 0.4 for *Aedes aegypti*. Additionally, precipitation in the wettest month demonstrated a consistently negative impact when it was less than 200 mm. This negative effect weakened in the range of 200–370 mm and then transitioned to a positive effect. Above 370 mm, there was a sudden change, with the total effect becoming consistently negative. When population density was above 50 people·hm^{-2}, this variable exerted a positive relation with the occurrence of dengue.

In the analysis of interactions between factors influencing dengue hazard, we selected the top four contributing factors: the minimum temperature in the coldest month, habitat suitability of *Aedes albopictus*, habitat suitability of *Aedes aegypti*, and precipitation in the wettest month. The interaction effects between the minimum temperature in the coldest month and other driving factors were diverse and complex (Fig.

3g–i). A relatively high minimum temperature in the coldest month had a positive effect on the regional dengue hazard when the habitat suitability of *Aedes albopictus* was above 0.6, and a relatively low minimum temperature in the coldest month had a negative effect on the regional dengue hazard when the suitability value for *Aedes albopictus* was approximately less than 0.6. Notably, when the habitat suitability of *Aedes albopictus* ranged from 0 to 0.4, the negative impact of minimum temperature in the coldest month was consistently maintained (Fig. 3g). Moreover, when the minimum temperature in the coldest month was relatively high (>0°C), the precipitation in the wettest month consistently exhibited a negative effect. This negative effect followed an inverted "U-shaped" pattern, where the effect initially increased and then decreased as the precipitation in the wettest month increased from 0 to 400 mm (Fig. 3i). Conversely, when the minimum temperature in the coldest month was low (<-10°C), an increase in precipitation in the wettest month led to a stable positive effect.

The spatial Shapley values revealed spatial disparities in the impacts of different variables on dengue hazard, with distinctive spatial patterns observed throughout China (Fig. 3m–p). For example, this was evident in the positive impact of the minimum temperature in the coldest month across Central South China and the negative impact of the minimum temperature in the coldest month across Northeast China and Northwest China (Fig. 3m). In most parts of East China and Central South China, the habitat suitability of both *Aedes albopictus* and *Aedes aegypti* had positive effects on the regional dengue hazard; however, in Northeast China and Northwest China, these effects and

negligible effects, respectively (Fig. 3n, o). Moreover, the precipitation in the wettest month exhibited positive contributions in Yunnan Province, and negative contributions were observed in Central South China and East China, with negligible contributions in all other regions (Fig. 3p). The dominant variables contributing to dengue occurrence were minimum temperature in the coldest month and the habitat suitability of *Aedes albopictus* in high-hazard areas of dengue. Additionally, we recognized the four factors with the highest Shapley values in each grid as the key factors that influence dengue hazard (Supplementary Figs. S6, S7).

Dengue risk assessment from a multidimensional perspective

Based on the hazard-exposure-vulnerability framework, we integrated human exposure, social vulnerability, and the regional dengue hazard to derive a spatially explicit dengue risk index (Figs. 4a-h and Fig. S8). The overall dengue risk highlighted notable regional disparities. High-risk areas were concentrated in southwestern China, Hainan Province, and the Shanghai and Shenzhen-Guangzhou metropolitan clusters. The spatial pattern of dengue hazard, human exposure, and social vulnerability indices collectively shaped the overall dengue risk (Figs. 4a, c, and e). The high dengue hazard values were clustered mainly in southwestern China, Hainan Province, and the Shenzhen–Guangzhou metropolitan cluster, reflecting frequent dengue events in these areas. High levels of human exposure were concentrated in densely populated regions, such as the Yangtze River Delta and the Pearl River Delta urban agglomeration, indicating that many

people may face a high probability of dengue infection in these areas. Areas of high social vulnerability, predominantly distributed in Southwest China and Northwest China, were associated with significantly aging populations, relatively limited sanitation facilities, or small per capita living spaces, suggesting a limited capacity to withstand or recover from dengue-related outbreaks.

Our research also identified the five counties with the highest dengue risk rankings in each geographical division. By analyzing how the dengue hazard, human exposure and social vulnerability levels jointly contributed to the overall dengue risk, we characterized the potential risk patterns across China (Fig. 4i). For example, some counties exhibited a pattern in which high dengue hazard levels were accompanied by dense populations yet comparatively moderate vulnerability, whereas other counties confronted the combined challenge of both high hazard levels and notable vulnerability, underscoring insufficient adaptive capacity (Supplementary Table S3, S4). Furthermore, we simulated dengue hazard, human exposure, and social vulnerability to determine dengue risk in 2050 and 2100, considering changes in only climate conditions, the habitat suitability of the *Aedes* vector, and the total population. The results indicated that the increase in dengue risk under the SSP585 high-emission scenario was the highest, with a 6.01% increase by 2050 and a 8.21% increase by 2100 (Supplementary Figs. S9-S12). Varying degrees of increase were also observed in other future scenarios. Notably, the increase in dengue risk exhibited spatial heterogeneity across geographical divisions. Overall, the dengue risk in all geographical divisions except Northeast China showed

increasing trends under the different SSP scenarios, with relatively greater increases observed in East China (12.02% by 2050 and 14.20% by 2100) and Central South China (4.16% by 2050 and 5.78% by 2100) in the SSP585 scenario than in other areas.

Field validation of GNNWLR-SHAP model for dengue hazard in Shenzhen City

To further validate the predictive accuracy of the GNNWLR-SHAP model for dengue hazard, we conducted targeted field validation in Shenzhen City using 2024 official dengue case records from the Shenzhen Center for Disease Control and Prevention (CDC) (Supplementary Note 6). This field validation showed the model achieved reliable predictive performance with an AUC of 0.888 (Table S9). The predicted spatial pattern of dengue hazard in Shenzhen was highly consistent with the actual distribution of confirmed cases (Fig. S22). High-hazard zones were concentrated in areas with dense population, intensive human mobility and high habitat suitability for Aedes mosquitoes. Spatial SHAP analysis further revealed that the minimum temperature of the coldest month (bio6) and habitat suitability of Aedes albopictus dominated dengue hazard in Shenzhen, and their spatially heterogeneous contributions matched the national-scale driving mechanism in this study (Figs. S23-S26). Collectively, these field validation results rigorously validate the robustness and practical applicability of the GNNWLR-SHAP model for regional dengue hazard prediction.

Discussion

In our study, a model (GNNWLR-SHAP) is developed to estimate regional dengue hazard level, and a multidimensional assessment framework (hazard-exposure-vulnerability) is introduced to systematically analyze the driving mechanisms and spatial evolution patterns of dengue risk across China. By integrating climatic factors, socioeconomic factors, and the habitat suitability of the *Aedes* vector, the dominant driving factors of the regional dengue hazard and their spatially heterogeneous contributions are quantitatively revealed. Moreover, the expansion trend of high-hazard areas of dengue in different future scenarios (SSP126, SSP245, and SSP585) is simulated. Furthermore, we couple the dengue hazard, population exposure, and social vulnerability through a risk assessment framework and identify "high hazard–high exposure–high vulnerability" composite risk hot spots. The spatial patterns of dengue risk are simulated across different future scenarios to clarify their spatiotemporal evolutionary trends.

The distribution of high-hazard areas of dengue in the current period indicates that persistent high dengue hazard levels are associated with year-round warm climates and a stable *Aedes* density in Southeast China and Southwest China, creating ideal conditions for local transmission. In the context of global warming, high-hazard areas of dengue have gradually expanded northward. The results obtained with the GNNWLR-SHAP model indicated that the temperature and habitat suitability of *Aedes* vectors significantly drove the expansion of high-hazard areas of dengue across China[28–30], although this process remained constrained by the actual ecological boundaries of *Aedes*

species[31,32]. This finding aligns with the biological mechanisms underlying dengue transmission, where temperature directly influences viral replication rates in *Aedes* vectors, adult *Aedes* survival rates, and the biting frequency[33,34]. These biological processes collectively influence the duration and intensity of dengue transmission[35]. For example, suitable temperatures (25–30°C) accelerate the virus incubation period in *Aedes* vectors, whereas extreme temperatures shorten the effective transmission window by suppressing *Aedes* survival or activity[36,37]. In addition to temperature, our findings align with previous research confirming that the presence of *Aedes aegypti* and *Aedes albopictus* is a prerequisite for local dengue transmission[38]. This was echoed by negligible dengue occurrence in regions lacking these *Aedes* vectors, even when other bioclimatic conditions were favorable. Most parts of Europe, characterized by a limited *Aedes* distribution, present low dengue hazard levels despite marginally ideal temperatures[39,40]. These findings highlight the urgent need to implement climate-adaptive *Aedes* control measures to mitigate dengue expansion in conjunction with global warming.

The interaction between temperature and precipitation should be considered to establish measures tailored to specific situations. In warm regions (minimum temperature in the coldest month > 0°C), the inverted “U-shaped" effect curve for the effect of precipitation on dengue hazard necessitates strengthened urban waterlogging control to prevent temporary water accumulation from excessive runoff[41]. During drought periods with insufficient precipitation, high-density patrols should be carried out for limited water sources to reduce the probability of human activities and mosquito contact around water

sources[42]. This bidirectional regulation strategy can effectively address the complex dengue hazards associated with the interactions between climate factors and enhance the environmental adaptability and cost-effectiveness of prevention and control measures.

Although climate and *Aedes* vector-related factors remain the fundamental influencers of the regional dengue hazard levels, the importance of socioeconomic factors (e.g., population density and urbanization) in increasing transmission probability cannot be overlooked. This amplification has occurred mainly through the increased frequency of human–mosquito contact and interaction, especially in regions with unplanned expansion and high urbanization rates. *Aedes* vectors are often attracted to areas of high population density, as unplanned urbanization often creates abundant artificial habitats and provides many potential breeding sites. Furthermore, poor socioeconomic conditions, such as poor housing quality and limited sanitation facilities, further exacerbate the vulnerability of these regions. Critically, these socioeconomic drivers interact synergistically with climatic suitability-related factors; climate factors act as dengue transmission boundaries, but socioeconomic conditions significantly influence the threshold for outbreaks within these boundaries. Therefore, sustainable dengue control must be combined with socioeconomic intervention measures, such as investing in equitable urban planning, improving housing, and helping high-hazard communities strengthen their adaptive capacity.

The spatial Shapley values revealed the heterogeneous impact of the driving factors on dengue hazard, underscoring the need for location-specific interventions. Temperature

acted as the dominant driver, with a critical tipping point at 0°C, below which *Aedes* survival and local dengue transmission were significantly suppressed. In Central South China, where temperature has a positive Shapley value (Fig. 3m), control measures such as mosquito breeding management during low-temperature periods (0–10°C) should be prioritized. In contrast, temperature had a negative effect in Northeast China and Northwest China, and low temperatures (-10–0°C) inherently suppress the activity of the *Aedes*·vector. The regional differences in the habitat suitability of *Aedes* vectors also provide a basis for guiding dengue control[14]. In East China and Central South China, where the habitat suitability of *Aedes* vectors has positive effects on dengue hazard (Fig. 3n, o), strategies should prioritize reducing *Aedes* habitats. For example, larvicides can be deployed, and environmental remediation can be carried out in areas where the habitat suitability level exceeds the critical point to disrupt the mosquito breeding chain[43,44]. In Yunnan Province, where precipitation has positive effects on dengue hazard, sustainable drainage systems and post-rainfall water management are critical to prevent mosquito breeding in residual pools, especially when precipitation is between 200–370 mm. These spatially heterogeneous impacts highlight that dengue prevention and control should be grounded in regional climate characteristics, vector ecology, and other conditions, necessitating precision-targeted, locally tailored interventions.

Further comparative analysis of spatial Shapley values revealed heterogeneously dominant driving factors in local regions. For regions dominated by high population density (> 50 people·hm^{-2}), the positive impact on dengue hazard necessitates

interventions to reduce human–mosquito contact, such as improving housing ventilation to minimize biting opportunities and implementing community surveillance for early outbreak detection. These spatially differentiated strategies not only avoid the inefficient allocation of resources in areas with low dengue potential but also support precise interventions targeting transmission drivers in different regions, embodying the logic of site-specific dengue prevention and control.

This study confirms that the essence of dengue risk lies in the dynamic balance between climatic suitability and social response capacity through the hazard-exposure-vulnerability framework[21]. For example, Yunnan and Hainan have long been identified as climatically suitable for persistent *Aedes* vectors[12]. The high dengue risk in these areas stems not only from warm temperatures meeting the *Aedes* survival threshold but also from the overlapping effects of climatic conditions and social vulnerability factors, such as aging populations and scarce healthcare resources, forming "vulnerability hotspots" with significantly limited adaptive capacity. Scarce healthcare resources indirectly exacerbate dengue vulnerability hotspots, primarily by limiting capacity for intervention for severe cases, early risk stratification, and rapid outbreak containment, rather than through direct prevention or cure of infection.

This multidimensional perspective also revealed counterintuitive trends, such as the high overall risk in the Yangtze River Delta driven primarily by exposure (e.g., large transient populations) and social vulnerability (e.g., aging rates > 20%), rather than the dengue hazard level alone. These insights challenge the assumption that dengue risk is

solely an ecological phenomenon and highlight the need for policies that address systemic inequities. For example, in remote rural areas, we can establish dengue prevention and control schemes targeting elderly individuals, train village doctors to provide home-based protection guidance, and thus alleviate social vulnerability. In megacities, an intelligent monitoring system for migrant population trajectories and dengue can be constructed to generate real-time dengue early warning maps for high-risk communities, thereby reducing potential dengue hazards. Compared with traditional risk assessment (simply quantifying the risk of dengue fever based on population in areas with high dengue hazard), the hazard-exposure-vulnerability framework provides site-specific decision support for dengue control, ensuring that interventions are both scientifically grounded and context specific. This promotes a comprehensive understanding of the patterns influencing health risks from the perspective of environmental exposure, reflecting the heterogeneity of dengue risk across China.

In all the climate scenarios, the overall dengue risk is simulated to gradually increase over the period of 2050–2100, with a spatially heterogeneous increase, especially in South China and Northwest China. This spatial heterogeneity might be attributed to the combined effects of climate-induced environmental changes and regional socioeconomic disparities. For example, the warm and humid climate under projected scenarios in South China could further extend the *Aedes* vector's activity period and geographic range, whereas increased habitat suitability for *Aedes* may occur in Northwest China owing to rising temperatures and altered precipitation patterns. Socioeconomic disparities, such

as aging populations and limited healthcare access in Southwest China or rapid urbanization with inadequate sanitation in Northwest China, exacerbate local vulnerability to dengue outbreaks. These combined factors create "high hazard–high vulnerability" hotspots in South China and emerging risk zones in Northwest China, where adaptive capacity remains insufficient to counter climate-driven transmission risks. Based on these findings, policymakers must prioritize adaptive strategies that account for the nuanced spatial trends identified in local areas.

Our study addresses the limitations of global dengue risk models through three major improvements. Methodologically, unlike traditional AI models such as Boosted Regression Tree and Maximum Entropy, which rely on global average effects and overlook regional heterogeneity, our GNNWLR-SHAP framework integrates geographic neural networks and SHAP values to identify China-specific thresholds. In terms of risk assessment, the study moves beyond the binary climate-vector framework by establishing a national hazard-exposure-vulnerability model that captures the unequal distribution of medical resources in China. Regarding mechanism analysis, the use of impervious surface area enables quantification of urbanization’s micro-scale influence on Aedes breeding, and the identification of temperature thresholds corrects the overestimation of dengue risk in northern China, thus providing scientifically grounded guidance for localized dengue prevention policies.

Despite its promise, the dengue risk assessment framework in our study is not without certain limitations. The most prominent one is the scale mismatch issue in habitat

suitability modeling. The assessment relies on macro-climatic data to simulate the habitat suitability of Aedes mosquitoes, yet overlooks microhabitat changes brought about by urbanization (e.g., building characteristics, artificial stagnant water patterns). This oversight makes it impossible to effectively identify mosquito breeding hotspots in urban microhabitats. We also fully acknowledge that a formal out-of-China external validation (e.g., in Southeast Asia) is still lacking at this stage. We have added this as an explicit limitation and outlined it as a priority direction for future work once suitable data become available. Furthermore, dengue hazard modeling relies on macro-climatic data and overlooks microhabitat changes caused by urbanization. The model does not fully consider biological interactions between vectors and pathogens, which may underestimate the moderating effect of biological factors on transmission efficiency. The resulting hazard maps should therefore be interpreted as serotype-agnostic estimates of overall dengue transmission potential. They do not distinguish between specific DENV serotypes or capture short-term serotype replacement dynamics, which must be assessed using local virological surveillance.

Additionally, the spatiotemporal evolution of social vulnerabilities (e.g., aging populations and unequal access to healthcare) might be overlooked, thus leading to a disconnect between static assessments and the dynamic reality of virus transmission. This further includes the lack of integration of individual-level population susceptibility factors, which may limit the model's ability to capture the nuanced regulation of these factors on transmission efficiency and severity. In future research, we plan to integrate

longer-term county-level socioeconomic panel data to construct a dynamic social vulnerability assessment model. This will further improve the hazard-exposure-vulnerability framework, enabling more accurate capture of the correlation mechanism between virus transmission and the dynamic evolution of social systems, and providing more targeted scientific support for regional dengue prevention and control strategies. While our model captures post-import diffusion via domestic mobility, it cannot directly integrate international travel flows due to data access constraints. This may lead to underestimation of import risk in border hubs with high international passenger volume. Future research will prioritize collaboration with public health authorities to access de-identified entry health declaration data, enabling direct quantification of international import risk and its integration into the hazard model. Notably, a key limitation of this study is that robust future projections of human vulnerability could not be established due to sparse temporal socioeconomic data (only 2010 and 2020 census records), the lack of validated downscaling methods for global SSP scenarios, and trend distortions caused by the COVID-19 pandemic. Collectively, these limitations highlight the need for future research to incorporate fine-scale microhabitat data and dynamic transmission pathways, enhancing the accuracy of dengue hazard estimations and the effectiveness of targeted interventions.

Conclusion

In conclusion, our study underscores the significant effects of climate factors and

socioeconomic factors on dengue risk through multiple mechanisms, such as temperature thresholds for *Aedes* survival, precipitation patterns, and human-vector contact intensity. Although short-term interventions such as targeted vector control and surveillance of imported cases can alleviate immediate transmission, the long-term northward expansion of high-hazard areas of dengue also requires sustained adaptation strategies under different warming and rapid urbanization scenarios. Therefore, integrated assessments and spatially explicit management schemes are essential, requiring collaboration among climate scientists, public health officials, and urban planners. Focus should be placed on regions with high "hazard-exposure-vulnerability" overlap, such as Southwest China and megacity clusters, which face compounded risks but often have uneven resource allocation patterns. Efforts must prioritize supporting these areas by implementing adaptive measures, such as climate-informed early warning systems and social vulnerability reduction programs. Addressing the complex interplay among climate dynamics, urbanization, and dengue transmission necessitates continuous research, policy innovation, and cross-sectoral coordination. A multipronged, collaborative approach is pivotal for effectively managing dengue risk and strengthening global public health resilience to climate-sensitive vector-borne diseases.

Data availability

Data for *Aedes* vector records are available via Github at https://github.com/Geoguang/Dengue-risk-assessment/tree/main. Dengue case records are openly available at https://doi.org/10.5281/zenodo.7765309. Data for the driving factors are provided in the Supporting Information.

Code availability

All analyses were conducted using python (version 3.9.18). The codes for this study are available at https://doi.org/10.5281/zenodo.19561940[56].

References

1. Ni, H. *et al.* Epidemiological characteristics and transmission dynamics of dengue fever in China. *Nat. Commun.* **15**, 8060 (2024).

2. Lin, Y., Fang, K., Zheng, Y., Wang, H. & Wu, J. Global burden and trends of neglected tropical diseases from 1990 to 2019. *J. Travel Med.* **29**, taac031 (2022).

3. World Health Organization. Special programme for research and training in tropical diseases. *Global Vector Control Response 2017-2030*. (World Health Organization, Geneva, 2017).

4. Deng, J. *et al.* Global, regional, and national burden of dengue infection in children and adolescents: an analysis of the Global Burden of Disease Study 2021.

eClinicalMedicine **78**, 102943 (2024).

5. Li, C. *et al.* Projecting future risk of dengue related to hydrometeorological conditions in mainland China under climate change scenarios: a modelling study. *Lancet Planet. Health* **7**, e397–e406 (2023).

6. Venkatesan, P. Global upsurge in dengue in 2024. *Lancet Infect. Dis.* **24**, e620 (2024).

7. Burki, T. Risk of dengue spread is high globally, says WHO. *Lancet Infect. Dis.* **24**, e161–e162 (2024).

8. The Lancet. Dengue: the threat to health now and in the future. *The Lancet* **404**, 311 (2024).

9. Kraemer, M. U. G. *et al.* Past and future spread of the arbovirus vectors *Aedes aegypti* and *Aedes albopictus*. *Nat. Microbiol.* **4**, 854–863 (2019).

10. Iwamura, T., Guzman-Holst, A. & Murray, K. A. Accelerating invasion potential of disease vector *Aedes aegypti* under climate change. *Nat. Commun.* **11**, 2130 (2020).

11. Li, R. *et al.* Climate-driven variation in mosquito density predicts the spatiotemporal dynamics of dengue. *Proc. Natl. Acad. Sci.* **116**, 3624–3629 (2019).

12. Messina, J. P. *et al.* The current and future global distribution and population at risk of dengue. *Nat. Microbiol.* **4**, 1508–1515 (2019).

13. Weaver, S. C. Urbanization and geographic expansion of zoonotic arboviral diseases:

mechanisms and potential strategies for prevention. *Trends Microbiol.* **21**, 360–363 (2013).

14. Cao, B. *et al.* Tracing the future of epidemics: Coincident niche distribution of host animals and disease incidence revealed climate-correlated risk shifts of main zoonotic diseases in China. *Glob. Change Biol.* **29**, 3723–3746 (2023).

15. Li, C. *et al.* Interaction of climate and socio-ecological environment drives the dengue outbreak in epidemic region of China. *PLoS Negl. Trop. Dis.* **15**, e0009761 (2021).

16. Lu, X. *et al.* Species-specific climate suitable conditions index and dengue transmission in Guangdong, China. *Parasit. Vectors* **15**, 342 (2022).

17. Ju, X. *et al.* How air pollution altered the association of meteorological exposures and the incidence of dengue fever. *Environ. Res. Lett.* **17**, 124041 (2022).

18. Johansson, M. A., Dominici, F. & Glass, G. E. Local and global effects of climate on dengue transmission in Puerto Rico. *PLoS Negl. Trop. Dis.* **3**, e382 (2009).

19. Sarma, D. K. *et al.* An assessment of remotely sensed environmental variables on dengue epidemiology in central India. *PLoS Negl. Trop. Dis.* **16**, e0010859 (2022).

20. Cheng, J. *et al.* Extreme weather conditions and dengue outbreak in Guangdong, China: Spatial heterogeneity based on climate variability. *Environ. Res.* **196**, 110900 (2021).

21. Yin, S. *et al.* Spatial pattern assessment of dengue fever risk in subtropical urban environments: The case of Hong Kong. *Landsc. Urban Plan.* **237**, 104815 (2023).

22. Kakarla, S. G., Bhimala, K. R., Kadiri, M. R., Kumaraswamy, S. & Mutheneni, S. R. Dengue situation in India: Suitability and transmission potential model for present and projected climate change scenarios. *Sci. Total Environ.* **739**, 140336 (2020).

23. Liu, K. *et al.* Facilitating fine-grained intra-urban dengue forecasting by integrating urban environments measured from street-view images. *Infect. Dis. Poverty* **10**, 40 (2021).

24. Oliveira, S., Capinha, C. & Rocha, J. Predicting the time of arrival of the Tiger mosquito (*Aedes albopictus*) to new countries based on trade patterns of tyres and plants. *J. Appl. Ecol.* **60**, 2362–2374 (2023).

25. Lippi, C. A. *et al.* Geographic shifts in *Aedes aegypti* habitat suitability in Ecuador using larval surveillance data and ecological niche modeling: Implications of climate change for public health vector control. *PLoS Negl. Trop. Dis.* **13**, e0007322 (2019).

26. Seposo, X., Valenzuela, S. & Apostol, G. L. Socio-economic factors and its influence on the association between temperature and dengue incidence in 61 provinces of the Philippines, 2010–2019. *PLoS Negl. Trop. Dis.* **17**, e0011700 (2023).

27. Do Carmo, R. F., Silva Júnior, J. V. J., Pastor, A. F. & De Souza, C. D. F. Spatiotemporal dynamics, risk areas and social determinants of dengue in

Northeastern Brazil, 2014–2017: an ecological study. *Infect. Dis. Poverty* **9**, 153 (2020).

28. Gwee, X. W. S. Global dengue importation: a systematic review. *BMC Infect. Dis.* **21**, 1078(2021).

29. Hales, S., De Wet, N., Maindonald, J. & Woodward, A. Potential effect of population and climate changes on global distribution of dengue fever: an empirical model. *The Lancet* **360**, 830–834 (2002).

30. Patz, J. A., Martens, W. J. M., Focks, D. A. & Jettend, T. H. Dengue fever epidemic potential as projected by general circulation models of global climate change. *Environ. Health Perspect.* **06**, (1998).

31. Brady, O. J. *et al.* Refining the global spatial limits of dengue virus transmission by evidence-based consensus. *PLoS Negl. Trop. Dis.* **6**, e1760 (2012).

32. Abdalgader, T., Banerjee, M. & Zhang, L. Spatially weak syncronization of spreading pattern between *Aedes albopictus* and dengue fever. *Ecol. Model.* **473**, 110123 (2022).

33. Feng, F. *et al.* Temperature-driven dengue transmission in a changing climate: Patterns, trends, and future projections. *GeoHealth* **8**, e2024GH001059 (2024).

34. Brady, O. J. *et al.* Modelling adult *Aedes aegypti* and *Aedes albopictus* survival at different temperatures in laboratory and field settings. *Parasit. Vectors* **6**, 351 (2013).

35. Lambrechts, L. *et al.* Impact of daily temperature fluctuations on dengue virus transmission by *Aedes aegypti*. *Proc. Natl. Acad. Sci.* **108**, 7460–7465 (2011).

36. Kaye, A. R. *et al.* The impact of natural climate variability on the global distribution of *Aedes aegypti*: a mathematical modelling study. *Lancet Planet. Health* **8**, e1079–e1087 (2024).

37. Mordecai, E. A. *et al.* Detecting the impact of temperature on transmission of Zika, dengue, and chikungunya using mechanistic models. *PLoS Negl. Trop. Dis.* **11**, e0005568 (2017).

38. Farooq, Z. *et al.* Impact of climate and *Aedes albopictus* establishment on dengue and chikungunya outbreaks in Europe: a time-to-event analysis. *Lancet Planet. Health* **9**, e374–e383 (2025).

39. Cattaneo, P. *et al.* Transmission of autochthonous *Aedes*-borne arboviruses and related public health challenges in Europe 2007–2023: a systematic review and secondary analysis. *Lancet Reg. Health - Eur.* **51**, 101231 (2025).

40. Medlock, J. M. *et al.* A review of the invasive mosquitoes in Europe: Ecology, public health risks, and control options. *Vector-Borne Zoonotic Dis.* **12**, 435–447 (2012).

41. Singh, A. A review of wastewater irrigation: Environmental implications. *Resour. Conserv. Recycl.* **168**, 105454 (2021).

42. Kearney, M., Porter, W. P., Williams, C., Ritchie, S. & Hoffmann, A. A. Integrating

biophysical models and evolutionary theory to predict climatic impacts on species' ranges: the dengue mosquito *Aedes aegypti* in Australia. *Funct. Ecol.* **23**, 528–538 (2009).

43. Cai, P. & Dimopoulos, G. Microbial biopesticides: A one health perspective on benefits and risks. *One Health* **20**, 100962 (2025).

44. Gómez, M., Martinez, D., Muñoz, M. & Ramírez, J. D. *Aedes aegypti* and *Ae. albopictus* microbiome/virome: new strategies for controlling arboviral transmission? *Parasit. Vectors* **15**, 287 (2022).

45. Zheng, X., Zhong, D., He, Y. & Zhou, G. Seasonality modeling of the distribution of *Aedes albopictus* in China based on climatic and environmental suitability. *Infect. Dis. Poverty* **8**, 98 (2019).

46. Liu, B. *et al.* Modeling the present and future distribution of arbovirus vectors *Aedes aegypti* and *Aedes albopictus* under climate change scenarios in Mainland China. *Sci. Total Environ.* **664**, 203–214 (2019).

47. Guang, X. Development and validation of a Geospatial eXplainable Artificial Intelligence (GeoXAI) framework for mapping mosquito density in metropolitans. *Appl. Geogr.* **181**, 103685 (2025).

48. Du, Z., Wang, Z., Wu, S., Zhang, F. & Liu, R. Geographically neural network weighted regression for the accurate estimation of spatial non-stationarity. *Int. J. Geogr. Inf.*

Sci. **34**, 1353–1377 (2020).

49. Wang, L. *et al.* Enhancing mineral prospectivity mapping with geospatial artificial intelligence: A geographically neural network-weighted logistic regression approach. *Int. J. Appl. Earth Obs. Geoinformation* **128**, 103746 (2024).

50. Kline, D. M. & Berardi, V. L. Revisiting squared-error and cross-entropy functions for training neural network classifiers. *Neural Comput. Appl.* **14**, 310–318 (2005).

51. Li, Z. Extracting spatial effects from machine learning model using local interpretation method: An example of SHAP and XGBoost. *Comput. Environ. Urban Syst.* **96**, 101845 (2022).

52. Brady, O. *et al.* The overlapping global distribution of dengue, chikungunya, Zika and yellow fever. *Nat. Commun.* **16**, 3418 (2024).

53. Aubrecht, C. & Özceylan, D. Identification of heat risk patterns in the U.S. National Capital Region by integrating heat stress and related vulnerability. *Environ. Int.* **56**, 65–77 (2013).

54. Chen, Q., Ding, M., Yang, X., Hu, K. & Qi, J. Spatially explicit assessment of heat health risk by using multi-sensor remote sensing images and socioeconomic data in Yangtze River Delta, China. *Int. J. Health Geogr.* **17**, 15 (2018).

55. Chen, J. *et al.* Improving the spatial prediction accuracy of soil alkaline hydrolyzable nitrogen using GWPCA-GWRK. *Soil Sci. Soc. Am. J.* **85**, 879–892 (2021).

56. Guang, X. *et al*. Custom computer code for 'Climate and socioeconomic factors drive heterogeneous dengue risk escalation in the Chinese population'. Zenodo. https://doi.org/10.5281/zenodo.19561940 (2026).

Funding

This study was funded by grants from the Prevention and Control of Emerging and Major Infectious Diseases-National Science and Technology Major Project (2025ZD01900800), Shenzhen Medical Research Fund (B2404002), Hainan Provincial Natural Science Foundation of China (326MS0423), and Shenzhen Science and Technology Program (JCYJ20240813095205008).

Acknowledgments

We would like to express my deepest gratitude to Professor Zijian Feng for his invaluable guidance during the conception and design stages of this research. His insightful feedback helped shape the direction of this work from the very beginning.

Author contributions

X.G. and B.Z. designed the study. X.G., Y.F.H., M.J.G., M.F.L., J.W., and D.F.K. collected the data. X.G., and Y.F.H. performed the modeling. X.G. wrote the first complete draft of the paper. Z.Z., L.B.X., L.Q.L., R.X.H., N.Z., F.A.C.P., C.M.R.V., C.M.L.S., P.L., and J.H.

contributed to the interpretation of the results and the writing and revision of the paper. H.D.W., J.L., and B.Z. revised the paper with inputs from all coauthors.

Competing interests

The authors declare that they have no competing interests.

Main text Figure captions

Fig. 1| Habitat suitability of *Aedes albopictus* and *Aedes aegypti* and the dengue hazard level in China in current and future scenarios. a–c, Spatial distributions of *Aedes albopictus*, *Aedes aegypti*, and dengue case records. **d–f,** Estimated habitat suitability of *Aedes albopictus* and *Aedes aegypti* and the dengue hazard level during the current period. **g–l,** The sum of the weighted latitudinal density distributions for the habitat suitability of *Aedes albopictus* and *Aedes aegypti* and the dengue hazard level in the current period, 2050, and 2100, with results colored according to the SSP scenario. Each future prediction (for 2050 and 2100) is based on three shared socioeconomic pathways (SSPs), which are scenarios of societal development used by the Intergovernmental Panel on Climate Change (IPCC), encompassing different trajectories of greenhouse gas emissions and concentrations: SSP126, SSP245, and SSP585. The habitat suitability value represents the probability that the *Aedes* vector can inhabit the area, varying between 0 (low suitability) and 1 (high suitability). The dengue hazard value represents the hazard level, which varies between 0 (low hazard level) and 1 (high hazard level).

Fig. 2| Changes in high-hazard areas for dengue by 2050 and 2100 under different future scenarios. a–c, Expansion (red) and contraction (blue) of high-hazard areas of dengue between the current year and 2050 under the SSP126, SSP245, and SSP585 scenarios. **d–f,** Expansion (red) and contraction (blue) of high-hazard areas of dengue between 2050 and 2100 under the SSP126, SSP245, and SSP585 scenarios. The dengue hazard level is categorized into five levels from highest to lowest: very high, high, moderate, low, and very low. The spatial distribution of the dengue hazard level is given in Supplementary Figs. S13 and S14. The hazard evolution rules are defined as follows: expansion: regions transitioning from very low/low levels to moderate/high/very high levels, and from moderate level to high/very high levels, indicating an escalation in the dengue hazard level; contraction: regions transitioning from high/very high levels to low/very low/moderate levels, and from moderate level to low/very low levels, reflecting a decline in the dengue hazard level; stable: regions with unchanged hazard levels, mutual transitions between low and very low levels, and mutual transitions between high and very high levels. **g,** Changes in the high-hazard areas of dengue at the six geographical division levels (Northeast China, Southwest China, North China, Northwest China, East China, and Central South China) and province-level regions by 2050 and 2100 are colored according to the SSP scenarios. The periods of 2050 and 2100 are shown in the left and right panels, respectively, and symbols denote negative and positive changes. A map of the six geographical divisions is given in Supplementary Fig. S15.

Fig. 3| Quantification of the Shapley additive explanation (SHAP) values of driving factors. a–l, Decomposition of the SHAP values of different features. SHAP total effects are decomposed into main effects, interaction effects, and remaining effects. **a–c,** SHAP total effects of the habitat suitability of *Aedes albopictus*, habitat suitability of *Aedes aegypti*, and bio13. SHAP total effects reflect the comprehensive impact of the habitat suitability of the *Aedes* vector and bio13 on dengue hazard, encompassing the combined effects of all factor combinations; **d–f,** SHAP main effects of the habitat suitability of *Aedes albopictus*, habitat suitability of *Aedes aegypti*, and bio13. SHAP main effects isolate the independent influences of individual driving factors on dengue hazard, excluding interactions between factors. **g–i,** SHAP interaction effects of bio6 with *Aedes albopictus*, *Aedes aegypti*, and bio13. SHAP interaction effects quantify the synergistic or antagonistic interactions between bio6 and other factors (i.e., habitat suitability of *Aedes albopictus*, habitat suitability of *Aedes aegypti*, and bio13); **j–l,** SHAP remaining effects. These remaining effects represent the cumulative interactions between bio6 and all other factors not explicitly analyzed, capturing residual influences not accounted for by main effects or pairwise interaction effects. **m–p,** Spatial distribution maps of SHAP values for bio6, habitat suitability of *Aedes albopictus*, habitat suitability of *Aedes aegypti*, and bio13. Note: bio6, minimum temperature in the coldest month; bio13, precipitation in the wettest month. The tipping point of each factor signifies the point at which the effect changed from negative to positive or from positive to negative.

Fig. 4| Maps for dengue risk assessment and the multidimensional components of risk in China at the county scale. a, c, e, g, Spatial distributions of human exposure, social vulnerability, dengue hazard level, and dengue risk level at the county scale. **b, d, f, h,** Percentages of counties with different levels of human exposure, social vulnerability, dengue hazard, and dengue risk. Red: very high level; light orange: high level; yellow: moderate level; light blue: low level; and blue: very low level. **i,** The top 5 counties ranked based on dengue risk and their hazard-exposure-vulnerability patterns in six geographical divisions (East China, Southwest China, Central South China, Northwest China, North China, and Northeast China) in China. A map of the six geographical divisions in China is given in Supplementary Fig. S15. The dengue risk index was derived via the equal-weight aggregation of three components (human exposure, social vulnerability, and dengue hazard level) obtained with the minimum–maximum normalization method. Green: human exposure index; purple: social vulnerability index; orange: dengue hazard index.

ED Summary

Guang, He, et al. establish a multi-dimensional dengue risk assessment framework that combines hazard, human exposure, and social vulnerability under climate change and rapid urbanization. They find a northward expansion of high-risk areas and identify integrated climate adaptation and urban planning

as key for prevention.

Peer review information: *Communications Medicine* thanks the anonymous reviewers for their contribution to the peer review of this work. A peer review file is available.

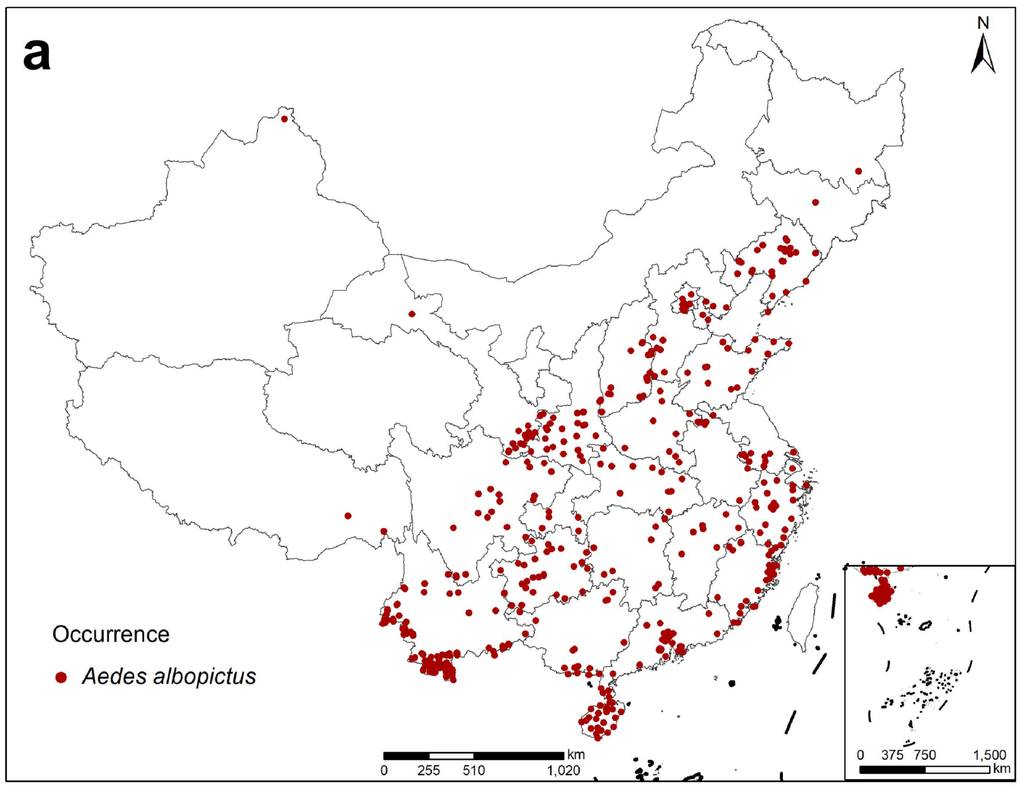
a
N
Occurrence
Aedes albopictus
0 255 510 1,020 km
0 375 750 1,500 km

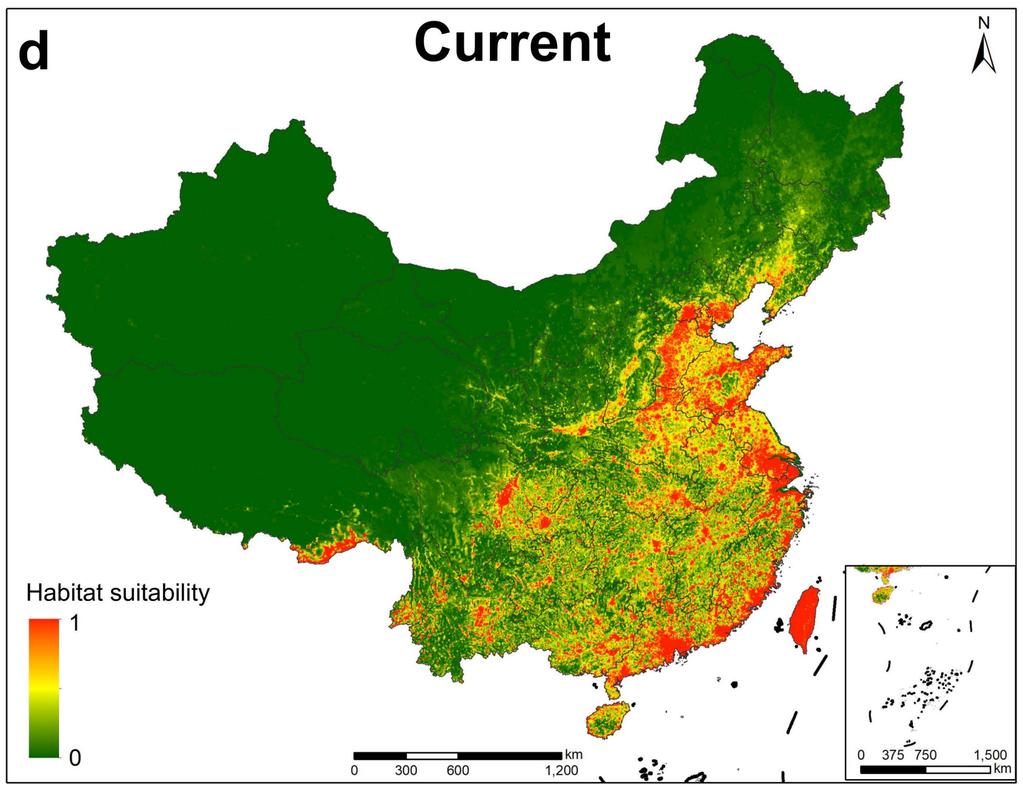
d
Current
N
Habitat suitability
1
0
0 300 600 1,200 km
0 375 750 1,500 km

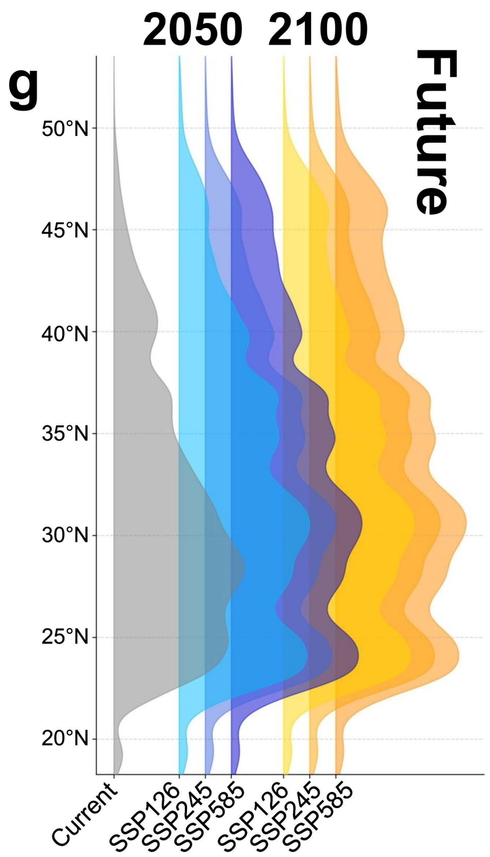
g
2050 2100
Future
50°N
45°N
40°N
35°N
30°N
25°N
20°N
Current
SSP126
SSP245
SSP585
SSP126
SSP245
SSP585

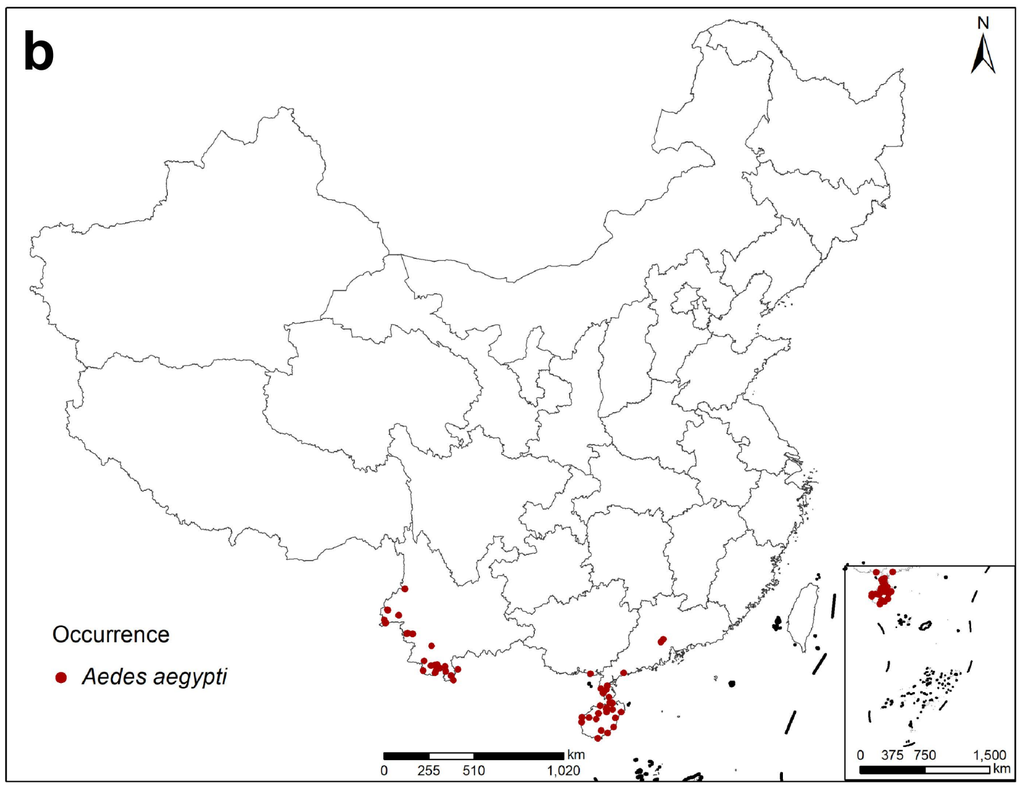
b
N
Occurrence
Aedes aegypti
0 255 510 1,020 km
0 375 750 1,500 km

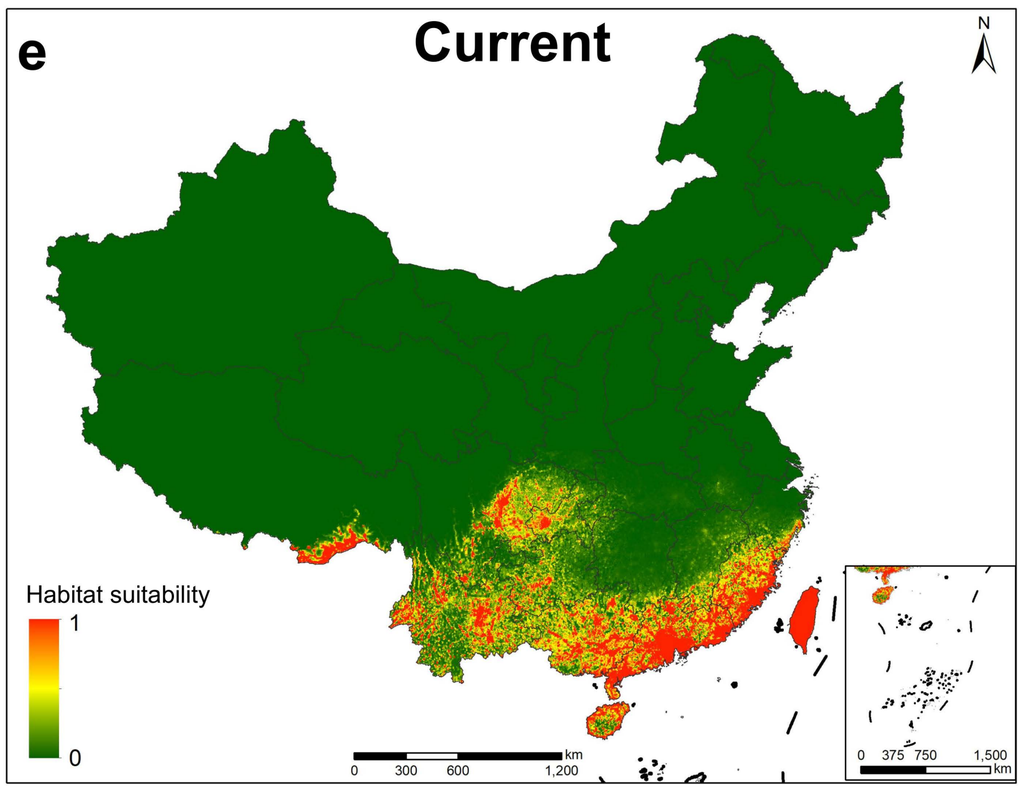
e
Current
N
Habitat suitability
1
0
0 300 600 1,200 km
0 375 750 1,500 km

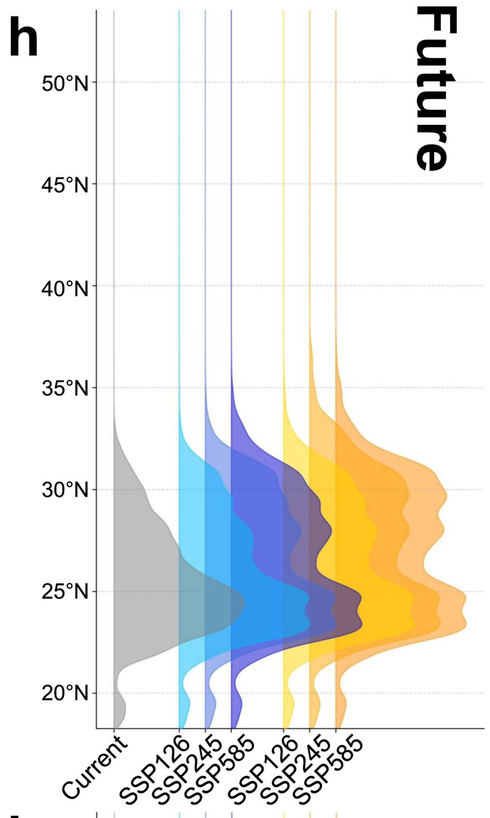
h
Future
50°N
45°N
40°N
35°N
30°N
25°N
20°N
Current
SSP126
SSP245
SSP585
SSP126
SSP245
SSP585

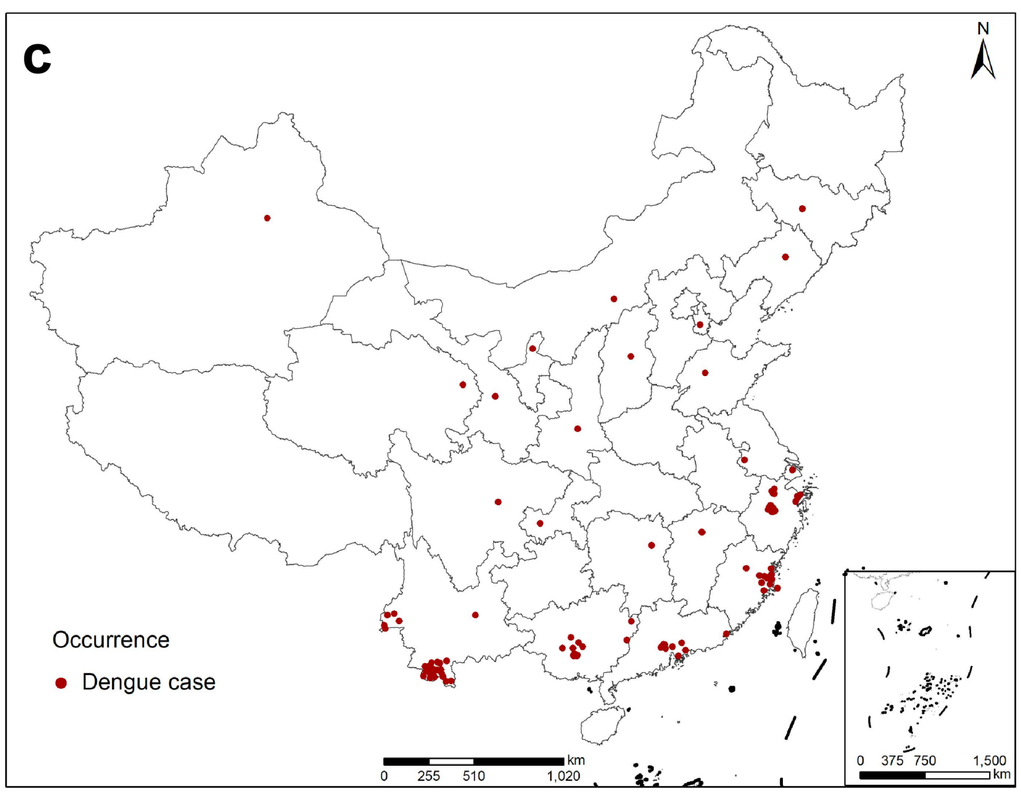
c
N
Occurrence
Dengue case
0 255 510 1,020 km
0 375 750 1,500 km

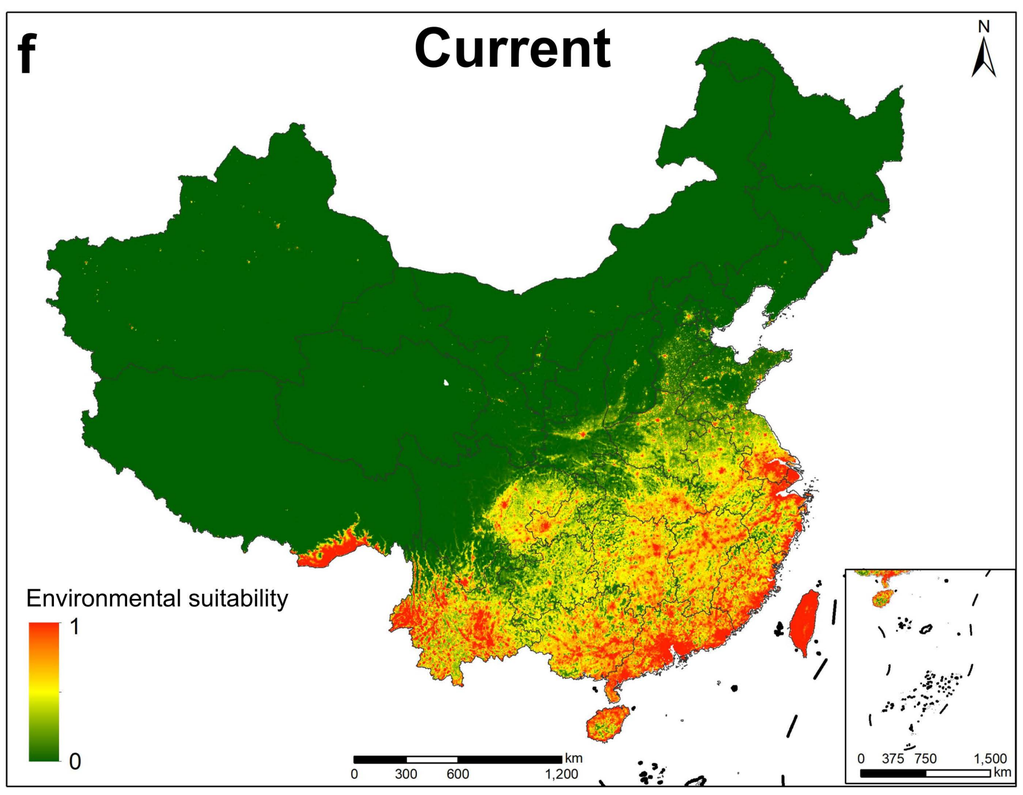
f
Current
N
Environmental suitability
1
0
0 300 600 1,200 km
0 375 750 1,500 km

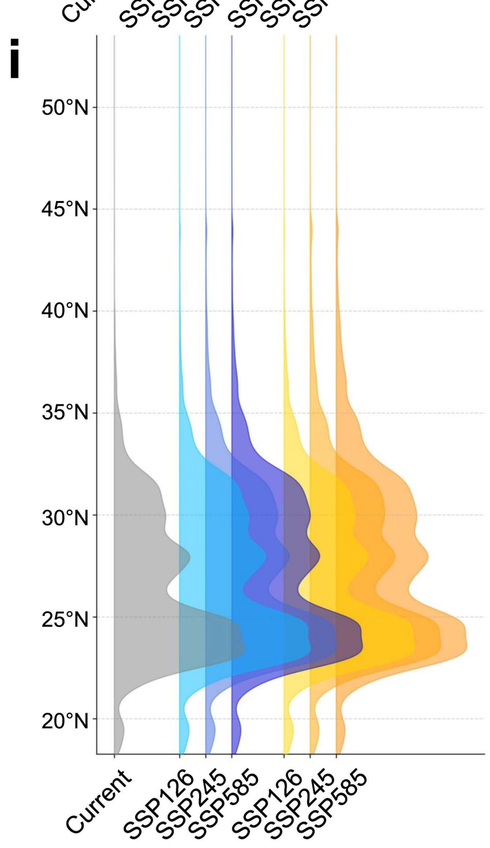
i
50°N
45°N
40°N
35°N
30°N
25°N
20°N
Current
SSP126
SSP245
SSP585
SSP126
SSP245
SSP585

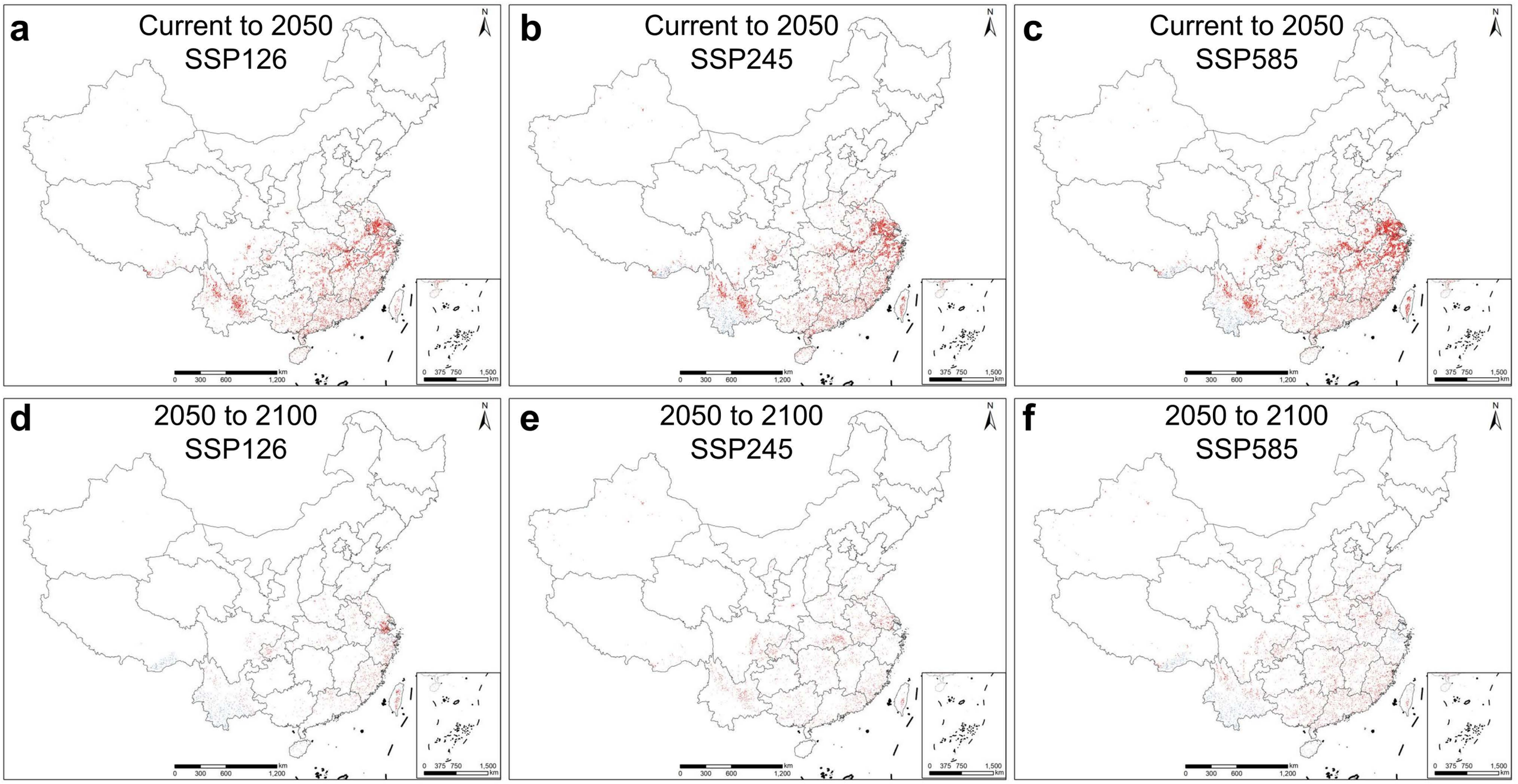
a
Current to 2050
SSP126
b
Current to 2050
SSP245
c
Current to 2050
SSP585
d
2050 to 2100
SSP126
e
2050 to 2100
SSP245
f
2050 to 2100
SSP585
N
0 300 600 1,200 km
0 375 750 1,500 km
Contraction
Stability
Expansion

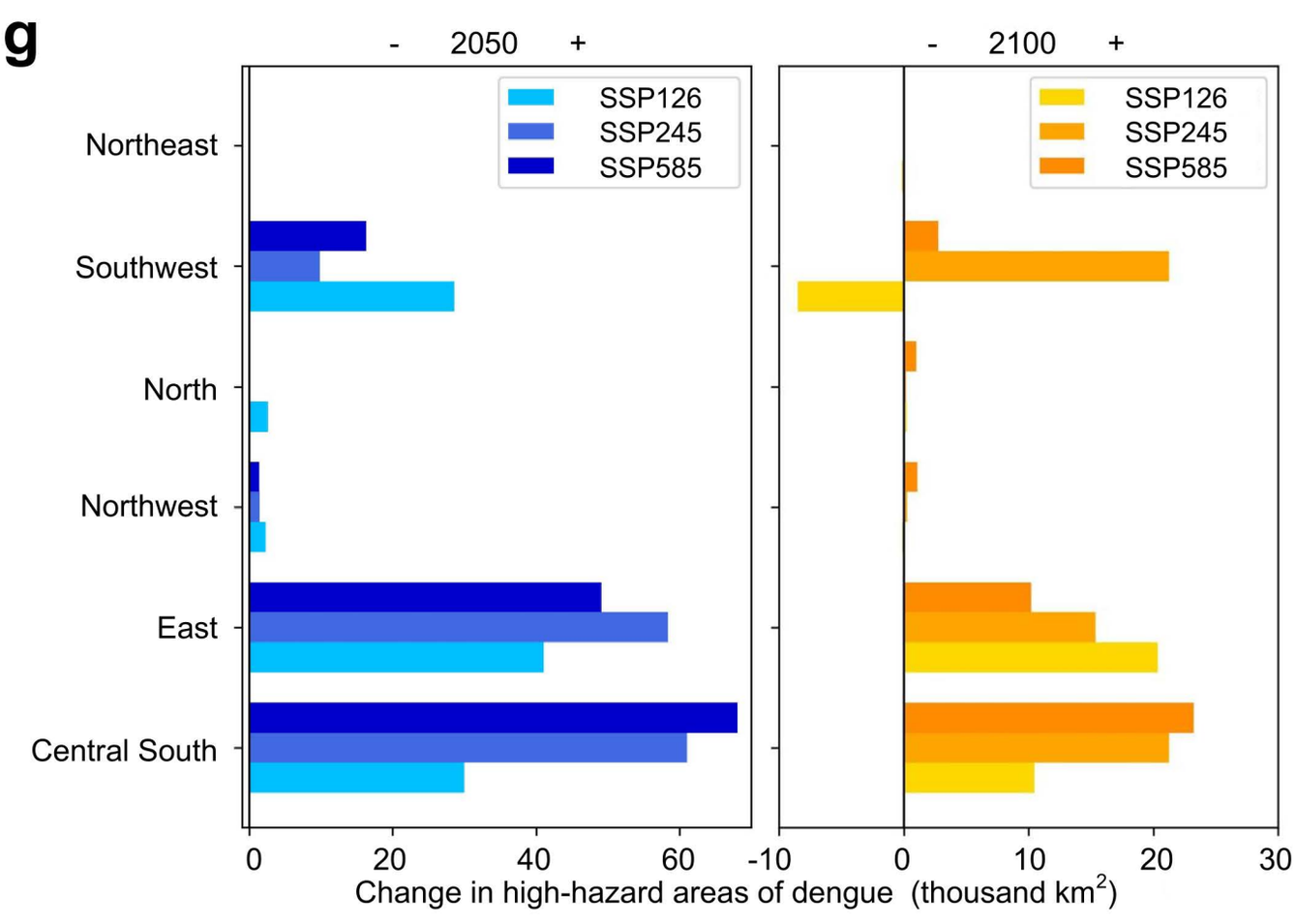
g
- 2050 +
- 2100 +
SSP126
SSP245
SSP585
Northeast
Southwest
North
Northwest
East
Central South
0 20 40 60
-10 0 10 20 30
Change in high-hazard areas of dengue (thousand km²)

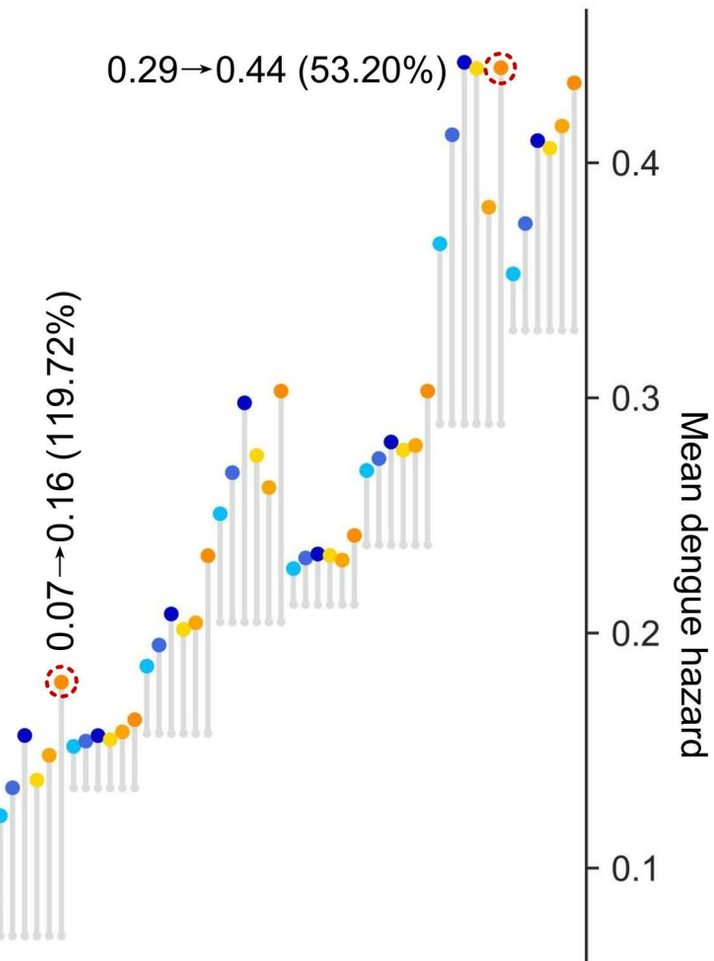
0.29→0.44 (53.20%)
0.03→0.08 (150.09%)
0.04→0.07 (68.92%)
0.06→0.10 (71.97%)
0.07→0.16 (119.72%)
0.0
0.1
0.2
0.3
0.4
Mean dengue hazard

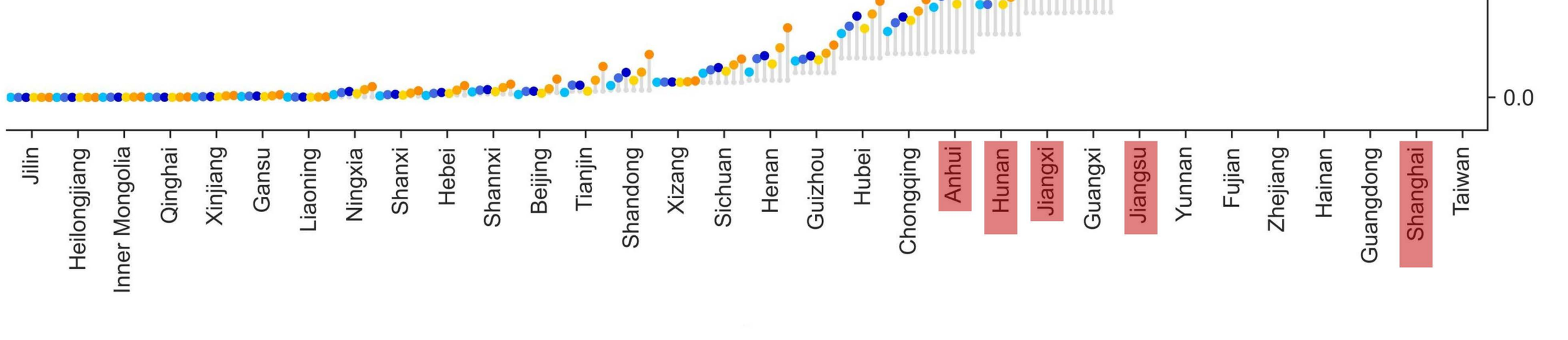
Jilin
Heilongjiang
Inner Mongolia
Qinghai
Xinjiang
Gansu
Liaoning
Ningxia
Shanxi
Hebei
Shannxi
Beijing
Tianjin
Shandong
Xizang
Sichuan
Henan
Guizhou
Hubei
Chongqing
Anhui
Hunan
Jiangxi
Guangxi
Jiangsu
Yunnan
Fujian
Zhejiang
Hainan
Guangdong
Shanghai
Taiwan

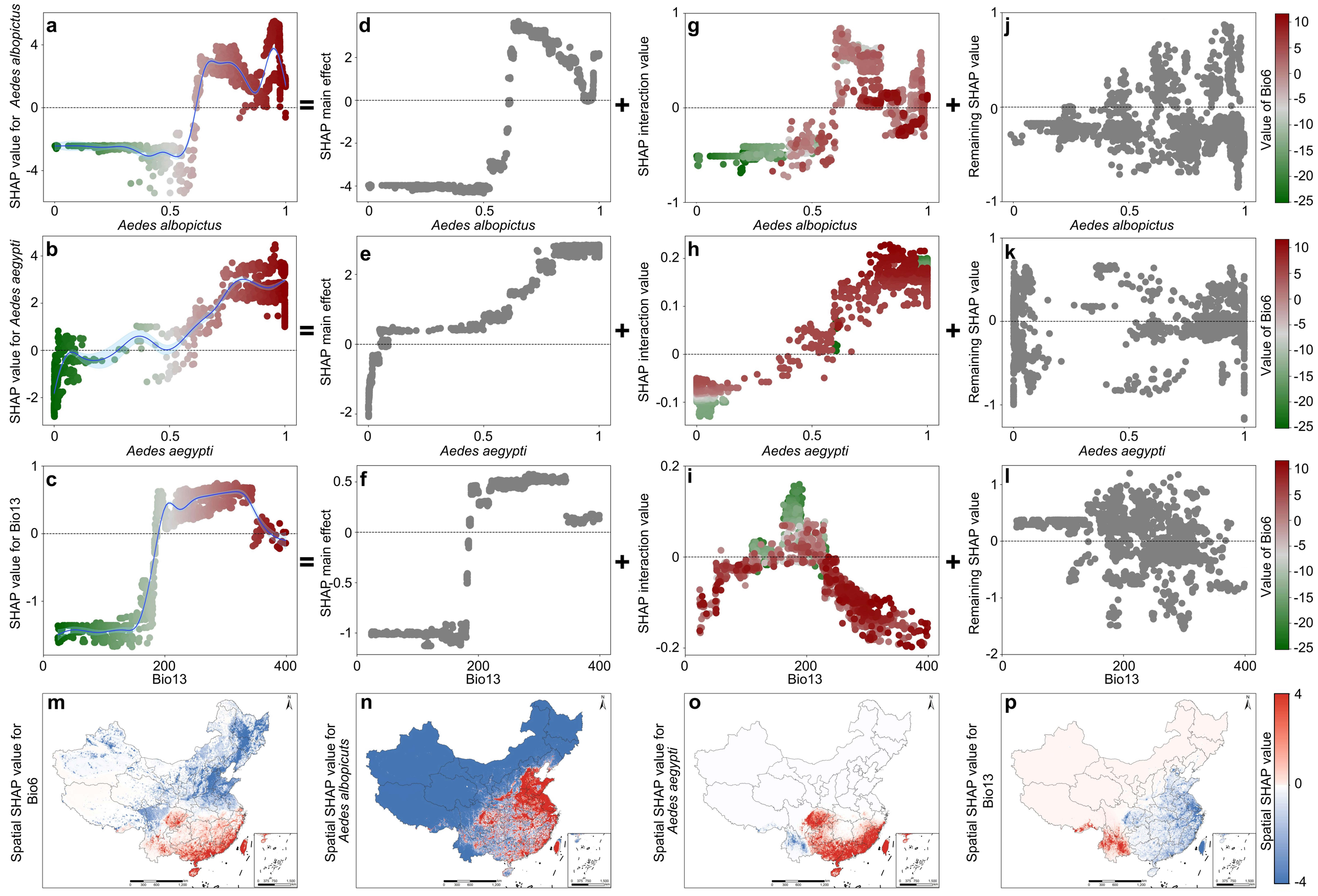
a
b
c
d
e
f
g
h
i
j
k
l
m
n
o
p
SHAP value for Aedes albopictus
SHAP value for Aedes aegypti
SHAP value for Bio13
SHAP main effect
SHAP interaction value
Remaining SHAP value
Aedes albopictus
Aedes aegypti
Bio13
Value of Bio6
Spatial SHAP value for Bio6
Spatial SHAP value for Aedes albopicuts
Spatial SHAP value for Aedes aegypti
Spatial SHAP value for Bio13
Spatial SHAP value
N

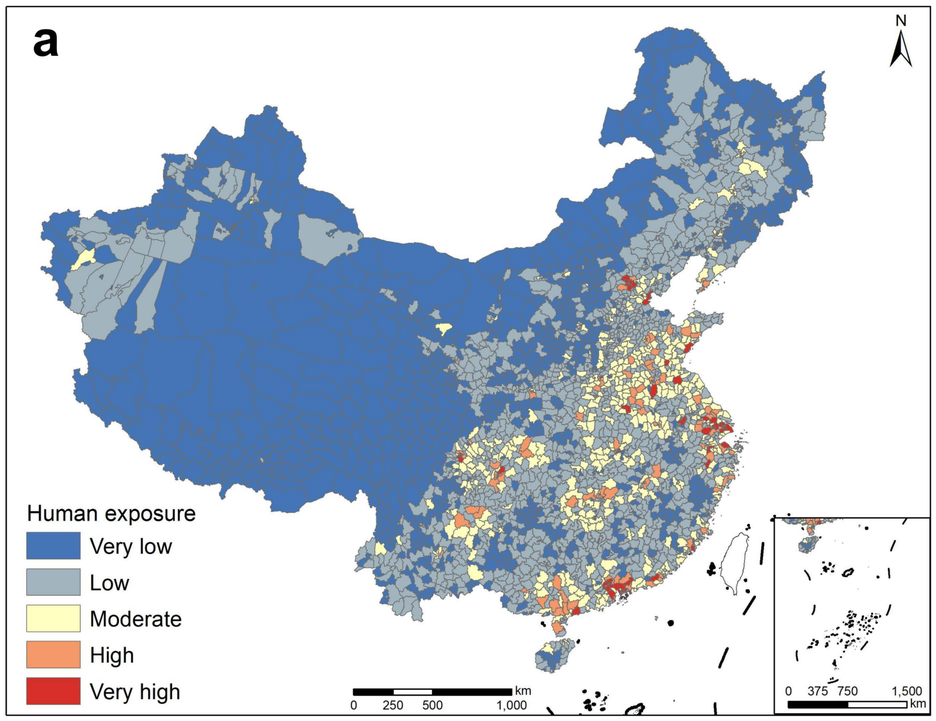
a
N
Human exposure
Very low
Low
Moderate
High
Very high
0 250 500 1,000 km
0 375 750 1,500 km

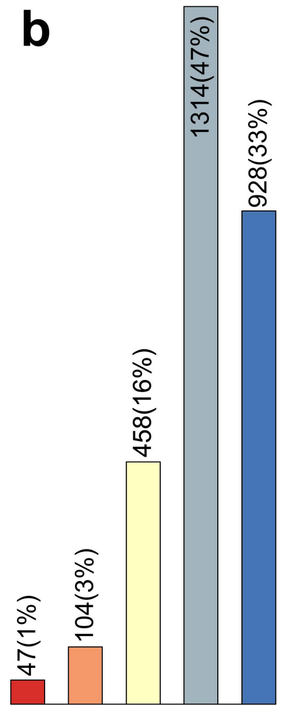
b
47(1%)
104(3%)
458(16%)
1314(47%)
928(33%)

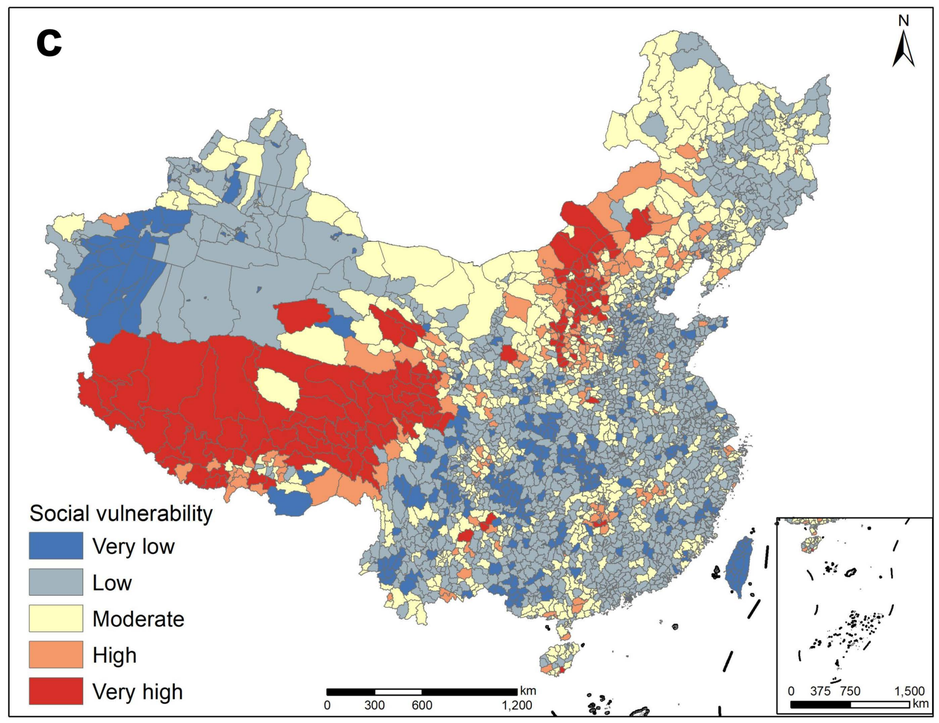
c
N
Social vulnerability
Very low
Low
Moderate
High
Very high
0 300 600 1,200 km
0 375 750 1,500 km

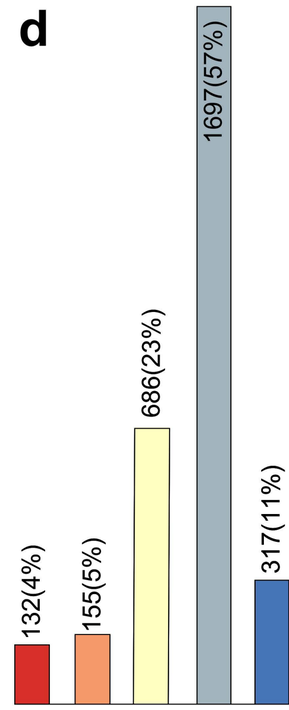
d
132(4%)
155(5%)
686(23%)
1697(57%)
317(11%)

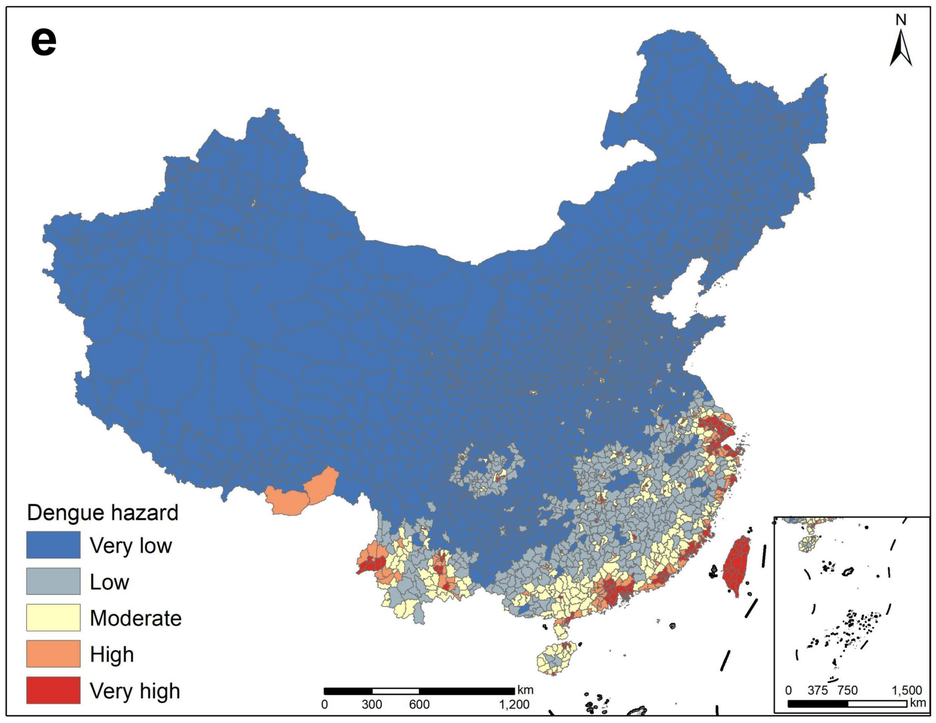
e
N
Dengue hazard
Very low
Low
Moderate
High
Very high
0 300 600 1,200 km
0 375 750 1,500 km

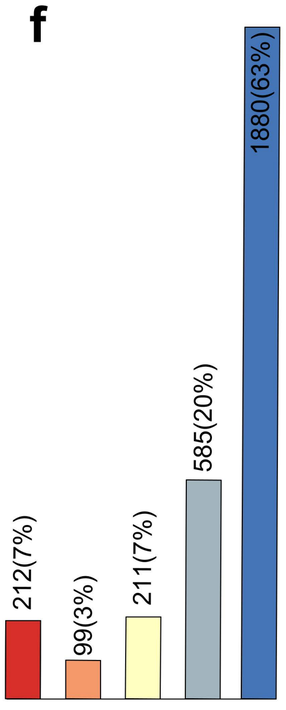
f
212(7%)
99(3%)
211(7%)
585(20%)
1880(63%)

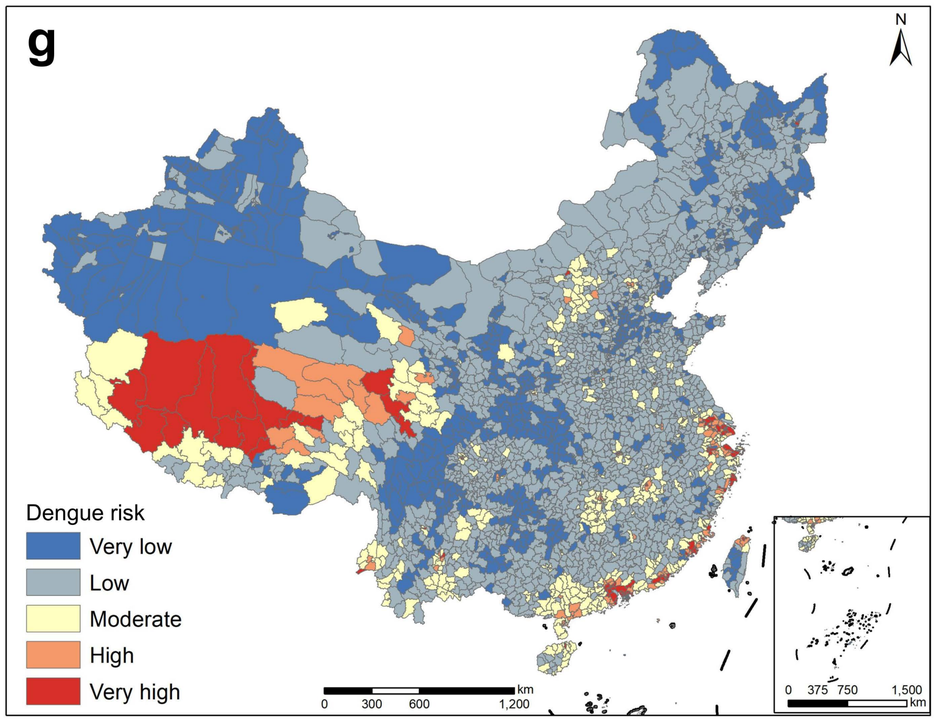
g
N
Dengue risk
Very low
Low
Moderate
High
Very high
0 300 600 1,200 km
0 375 750 1,500 km

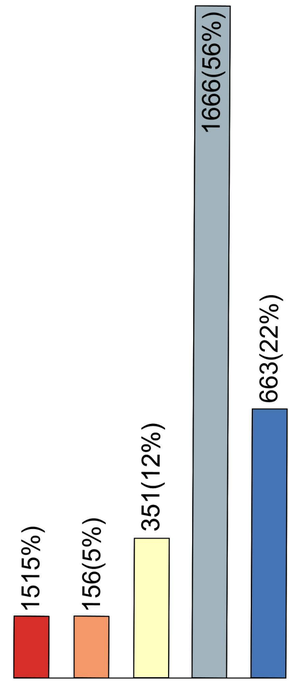
1515%)
156(5%)
351(12%)
1666(56%)
663(22%)

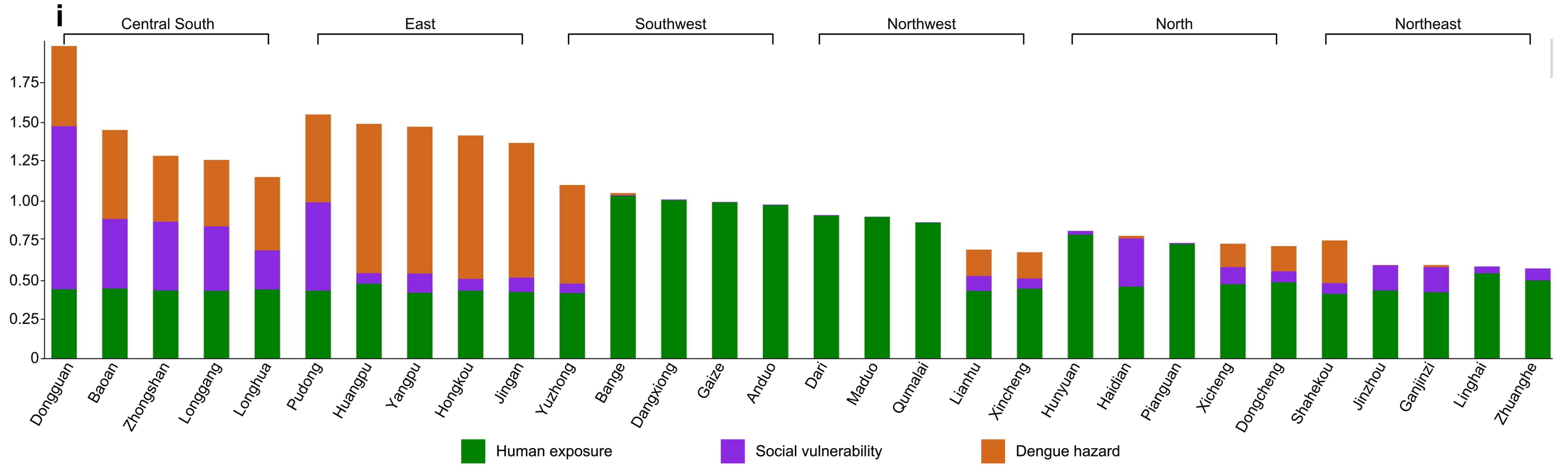
i
Central South
East
Southwest
Northwest
North
Northeast
1.75
1.50
1.25
1.00
0.75
0.50
0.25
0
Dongguan
Baoan
Zhongshan
Longgang
Longhua
Pudong
Huangpu
Yangpu
Hongkou
Jingan
Yuzhong
Bange
Dangxiong
Gaize
Anduo
Dari
Maduo
Qumalai
Lianhu
Xincheng
Hunyuan
Haidian
Pianguan
Xicheng
Dongcheng
Shahekou
Jinzhou
Ganjinzi
Linghai
Zhuanghe
Human exposure
Social vulnerability
Dengue hazard